Bulletin of the Seismological Society of America, Vol. 94, No. 4, pp. 1379–1401, August 2004

Interpretation of the Seattle Uplift, Washington, as a Passive-Roof Duplex

by Thomas M. Brocher, Richard J. Blakely, and Ray E. Wells

Abstract We interpret seismic lines and a wide variety of other geological and geophysical data to suggest that the Seattle uplift is a passive-roof duplex. A passive-roof duplex is bounded top and bottom by thrust faults with opposite senses of vergence that form a triangle zone at the leading edge of the advancing thrust sheet. In passive-roof duplexes the roof thrust slips only when the floor thrust ruptures. The Seattle fault is a south-dipping reverse fault forming the leading edge of the Seattle uplift, a 40-km-wide fold-and-thrust belt. The recently discovered, north-dipping Tacoma reverse fault is interpreted as a back thrust on the trailing edge of the belt, making the belt doubly vergent. Floor thrusts in the Seattle and Tacoma fault zones, imaged as discontinuous reflections, are interpreted as blind faults that flatten updip into bedding plane thrusts. Shallow monoclines in both the Seattle and Tacoma basins are interpreted to overlie the leading edges of thrust-bounded wedge tips advancing into the basins. Across the Seattle uplift, seismic lines image several shallow, short-wavelength folds exhibiting Quaternary or late Quaternary growth. From reflector truncation, several north-dipping thrust faults (splay thrusts) are inferred to core these shallow folds and to splay upward from a shallow roof thrust. Some of these shallow splay thrusts ruptured to the surface in the late Holocene. Ages from offset soils in trenches across the fault scarps and from abruptly raised shorelines indicate that the splay, roof, and floor thrusts of the Seattle and Tacoma faults ruptured about 1100 years ago.

Introduction

The Puget Lowland is a densely populated, seismically active lowland in the forearc of Washington's Cascadia convergent margin. Subduction is oblique, and basins making up the Lowland are separated by fault-bounded structural uplifts that accommodate margin parallel shortening at about 3–5 mm/yr (Wells *et al.*, 1998; Miller *et al.*, 2001; Hyndman *et al.*, 2003). The eastward-trending Seattle fault zone forms the northern flank of the Seattle uplift (Gower *et al.*, 1985; Yount and Gower, 1991). Johnson *et al.* (1994, 1999), Pratt *et al.* (1997), and ten Brink *et al.* (2002) interpreted seismic reflection lines as indicating that the fault zone is part of a regional, north-directed thrust system (Fig. 1). Seismic tomography and gravity inversions revealed structural relief decreasing westward along the fault (Brocher *et al.*, 2001), and aeromagnetic, geologic, and high-resolution seismic reflection data were subsequently used to map several strands of the Seattle fault zone (Blakely *et al.*, 2002).

Widespread uplift of up to 7 m of tidal marshes and marine terraces in the central Puget Lowland (Fig. 1) indicates that a large earthquake occurred on the buried Seattle fault about 1100 years ago (Bucknam *et al.*, 1992; Sherrod, 1998; Atwater, 1999). West of Puget Sound, airborne laser terrane mapping has revealed the presence of postglacial fault scarps along strands of the Seattle fault zone on Bainbridge Island (Fig. 1) and the adjacent Kitsap Peninsula (Nelson *et al.*, 2002, 2003a,b). These scarps all face southward, and trenches across three of the surface ruptures all indicate south-directed thrusting at the surface. This is surprising because the main Seattle fault is interpreted to be a south-dipping thrust fault in all of the published interpretations (referenced previously).

Along the southern boundary of the Seattle uplift, the SHIPS seismic data defined a large, north-dipping structure called the Tacoma fault zone (Brocher *et al.*, 2001; Parsons *et al.*, 2001; Van Wagoner *et al.*, 2002; Johnson *et al.*, 2004), and Brocher *et al.* (2001) suggested that the Seattle uplift is a structural pop-up bounded by the Seattle and Tacoma fault zones (Fig. 1). Sherrod *et al.* (2004) summarized fault-scarp evidence for north-side-up Holocene folding along the Catfish Lake scarp within the western Tacoma fault zone (Fig. 1).

In this article, we hypothesize a model to reconcile north-directed thrusting on the Seattle fault with the physiographic and paleoseismic evidence for dominantly south-directed Holocene thrusting at the surface. We explore the possibility that the shallow, southward-verging surface ruptures are rooted into a north-dipping roof thrust that merges with the Seattle fault in the subsurface. We hypothesize that

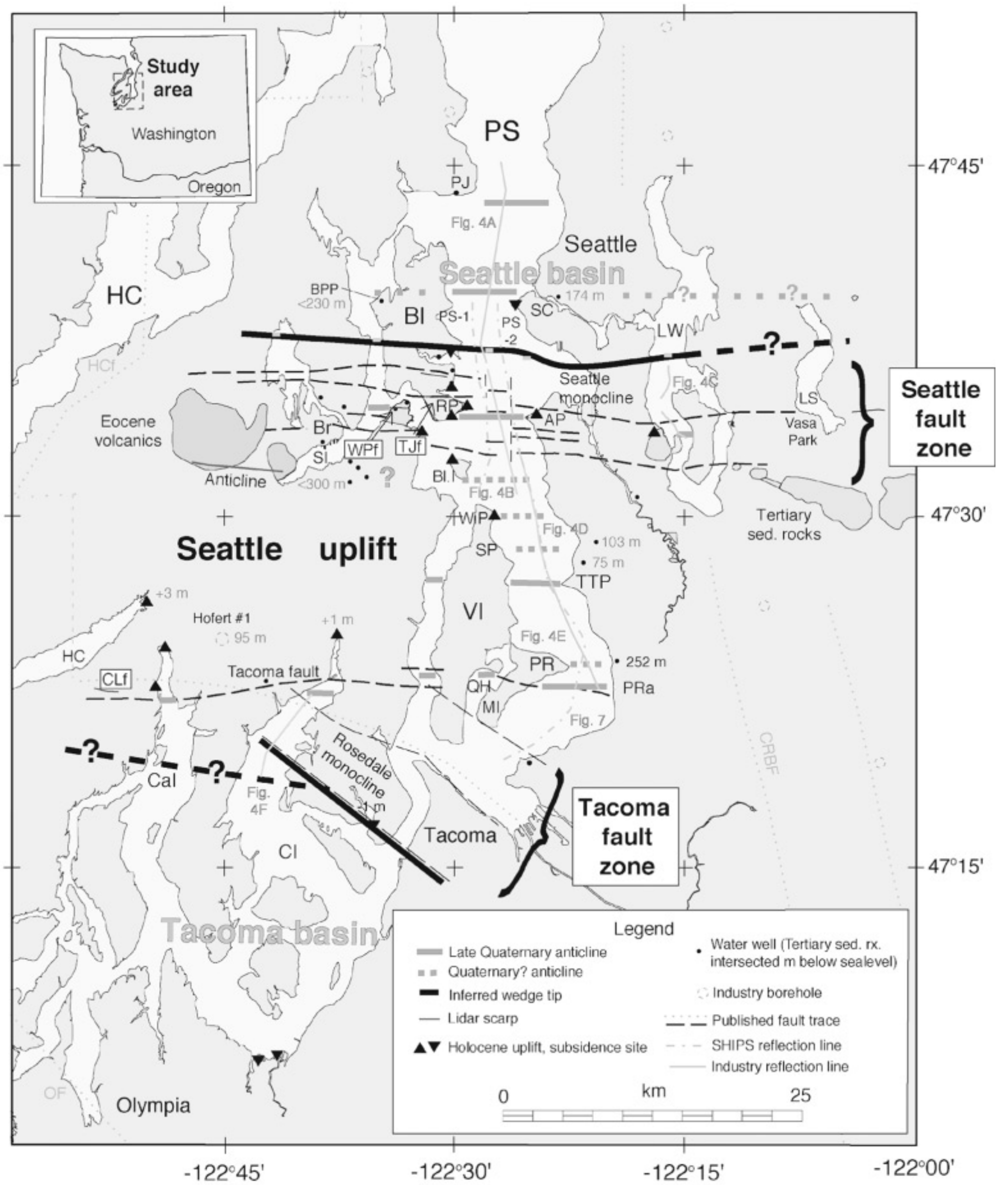

Figure 1. Mapped fault strands along the northern and southern flanks of the Seattle uplift (long black dashed lines) (Johnson *et al.*, 1999, 2004). Other inferred fault strands (gray dotted lines) are from Brocher *et al.* (2001) and Blakely *et al.* (2002). Locations of seismic lines shown in the figures are indicated as gray solid and dashed lines. Locations of subsurface wedge tips identified in the lines are shown as thick black lines and are dashed where projected. Black triangles show Holocene uplift sites and inverted black triangles show subsidence sites (Bucknam *et al.*, 1992; Sherrod, 1998, 2001; Sherrod *et al.*, 2004a). Thin black lines show either LIDAR or trenched Holocene fault scarps (Nelson *et al.*, 2002, 2003a,b; Sherrod *et al.*, 2003, 2004). Industry boreholes are indicated by dashed circles and selected water well locations by black filled circles with numbers indicating depth to Tertiary sedimentary rocks. Shaded areas west of Puget Sound show outcrops of Eocene volcanic rocks; shaded areas east of Puget Sound show outcrops of Tertiary sedimentary rocks (Yount and Gower, 1991). Abbreviations: AP, Alki Point; BI, Bainbridge Island; Bl.I, Blake Island; BPP, Battle Point Park; Br, Bremerton; CaI, Case Inlet; CI, Carr Inlet; CLf, Catfish Lake fault; CRBF, Coast Range Boundary fault; HC, Hood Canal; LS, Lake Sammamish; LW, Lake Washington; MI, Maury Island; OF, Olympia fault; PJ, Point Jefferson; PR, Point Robinson; PS, Puget Sound; RP, Restoration Point; SC, Ship Canal anticline; SI, Sinclair Inlet; SP, Seahurst Park; TJf, Toe Jam Hill fault; TTP, Three Tree Point; VI, Vashon Island; WiP, Winghaven Park; WPf, Waterman Point fault. Study location area shown in inset.

a triangle zone, which is bounded at top and bottom by thrust faults with opposite senses of vergence (Fig. 3C), characterizes both the Seattle and Tacoma fault zones. Such features are recognized in a number of fold and thrust belts elsewhere, and the responsible structures are described as passive-roof duplexes (e.g., Banks and Warburton, 1986; Jones, 1996b). We examine existing seismic reflection, aeromagnetic, and gravity data from the Seattle uplift and the adjacent Seattle and Tacoma fault zones to look for shallow monoclinal and locally divergent reflectors characteristic of triangle zones (Jones, 1996b). Data from the shallow, short-wavelength folds across the Seattle uplift are also examined to look for evidence of splay thrusting that might root into a shallow (1- to 2-km deep) roof thrust. If substantiated, the inferred splay, roof, and floor thrust geometry (Fig. 3C) along the Seattle uplift could have important implications for the analysis of seismic hazard between Seattle and Tacoma.

Seismic Reflection Data Quality, Constraints, and Caveats

Our interpretations are based on three different sets of marine multichannel seismic reflection lines. First, we interpreted oil industry lines described by Johnson *et al.* (1994) and Pratt *et al.* (1997). These lines were acquired using a variety of acquisition parameters down to 4- to 5-sec two-way travel time (twtt). Second, we examined high-resolution lines acquired by the USGS to 2-sec twtt (Johnson *et al.*, 1999, 2004). Last, we interpreted deep-crustal SHIPS lines (Fisher *et al.*, 1999) previously studied by Calvert *et al.* (2001, 2003), ten Brink *et al.* (2002), and Fisher *et al.* (2004).

Each set of seismic data has its own strengths and weaknesses. The oil industry lines generally have different acquisition and processing parameters, making some lines more readily interpretable than others. Their common-midpoint spacing (about 15.2 m) is larger than that for the SHIPS data (12.5 m). The USGS high-resolution lines provide greater spatial coverage than the industry lines and are helpful in mapping the wedge tips of the triangle zones along the Seattle and Tacoma faults. The SHIPS lines corroborate many features observed in the industry seismic lines and image the entire crust to 16-sec twtt (Fisher *et al.*, 2004).

Interpretation of these data is hampered by several factors, including the difficulty in imaging the subsurface using sparsely located profiles containing interfering multiple reflections and scattered coherent noise. The limitations of interpretations based on the existing seismic data, which are often old and acquired with suboptimal parameters, should be clearly recognized.

Surface geological mapping and borehole data provide sparse constraints on the interpretation of the seismic profiles. Outcrops of Tertiary sedimentary rocks and Eocene volcanic rocks are largely restricted to a narrow belt along the northern end of the Seattle uplift (Fig. 1) (e.g., Yount *et al.*, 1985; Yount and Gower, 1991; Haeussler and Clark, 2000; Blakely *et al.*, 2002). Deep borehole control is limited to the Kingston Arch, north of the Seattle basin, and to the Hofert #1 well (Fig. 1) along the Tacoma fault (McFarland, 1983; Brocher and Ruebel, 1998). Water wells intersected Tertiary sedimentary rocks in a few locations (e.g., Sceva, 1957; Buchanan-Banks and Collins, 1994; Jones, 1996a). Travel time versus depth curves calculated from sonic velocity logs in industry test holes (Brocher and Ruebel, 1998) and depth conversions of migrated seismic profiles based on SHIPS velocity models (ten Brink *et al.*, 2002) provide estimates of reflector depths

The seismic stratigraphy of the central lowland was summarized by Pratt *et al.* (1997) and Johnson *et al.* (1994; 1999) and has been described by Fulmer (1975), Yount and Gower (1991), and Rau and Johnson (1999). In the Seattle basin, Eocene Crescent Formation basalt is thought to form the basement beneath Eocene deep marine strata and younger sedimentary rocks of the late Eocene and Oligocene Blakeley and Miocene Blakely Harbor Formations, as well as largely unconsolidated Plio-Pleistocene deposits (Fig. 2).

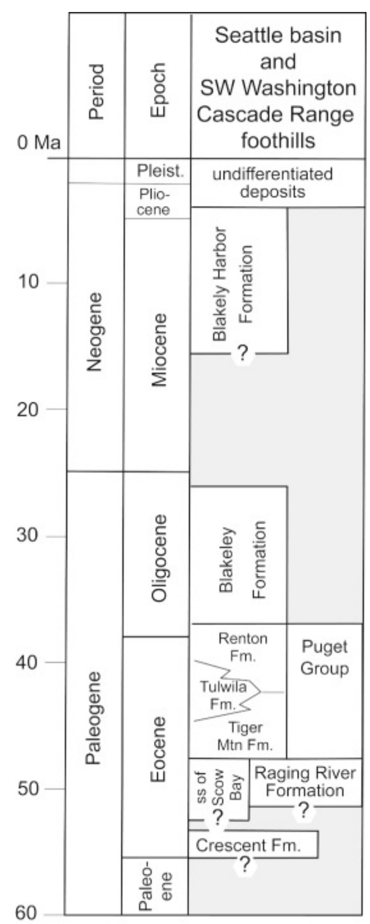

Figure 2. Stratigraphy described from boreholes in the Seattle basin and surrounding area, modified from Rau and Johnson (1999). Shaded areas show intervals of nondeposition and/or erosion.

The Late Eocene and Oligocene Blakeley Formation is largely composed of deep water turbidites (Johnson *et al.*, 1999). The nonmarine Upper Miocene Blakely Harbor Formation (Fulmer, 1975) likely records uplift starting about 15 m.y.a., possibly along the Seattle fault (ten Brink *et al.*, 2002).

Pleistocene glacial deposits in these data are normally either acoustically transparent or show highly discontinuous reflectors. Tertiary sedimentary rocks generate locally prominent, continuous reflections up to several kilometers in length. Although the contact at the top of the Eocene volcanic basement is strongly imaged, strata within the volcanic basement generally produce weak, discontinuous arrivals.

Interpretation of the Seismic Reflection Data

The structure of the Seattle fault zone varies dramatically along strike (Fig 1) (Brocher *et al.*, 2001; Blakely *et al.*, 2002; B. L. Sherrod *et al.*, unpublished manuscript 2004), but the deep seismic reflection lines are restricted to Puget Sound. Our interpretations based primarily on marine seismic reflection lines apply only to that part of the fault where evidence of south-facing surface ruptures is abundant. The tomography models (e.g., Brocher *et al.*, 2001) and the high-resolution seismic lines (Johnson *et al.*, 1999) allow us to generalize to some degree the structure away from Puget Sound, but comparable data are lacking for the far-eastern end of the uplift. The hanging wall of the Seattle fault zone contains folds oriented transverse to the fault and indicate a complex deformation history (Fig. 1). Given their short fold wavelengths and their tight fault spacing, structures imaged in the Puget Sound likely vary along strike. East of Seattle, at least one shallow, north-directed thrust has broken the surface (B. L. Sherrod *et al.*, unpublished manuscript, 2004), indicating changes in vergence along strike, similar to that observed in other thrust belts (Castonguay and Price, 1995). Most of the key features described in this report are best observed in proprietary industry seismic profiles (Fig. 4), but some are only recognized in USGS profiles (Johnson *et al.*, 1994, 1999; Pratt *et al.*, 1997; ten Brink *et al.*, 2002; Fisher *et al.*, 2004). Inconsistencies in the character of the reflections from the different data sources are sometimes problematic and permissive of quite different interpretations.

Seismic Evidence for a Triangle Zone Along the Seattle Fault Zone

We interpret the pronounced north-dipping monocline as forming the southern margin of the Seattle basin above a triangle zone along the leading edge of the Seattle fault zone. We informally name this monocline the Seattle monocline (Fig. 4C), because it is imaged both to the east and west of Seattle (Johnson *et al.*, 1999). Pratt *et al.* (1997) first recognized the monocline as an inflection (their axial surface F) in the Tertiary/Quaternary unconformity in the Seattle basin (Fig. 4A) and attributed it to fault-propagation folding (Fig. 3A). This monocline was subsequently imaged in the SHIPS reflection lines (Fig. 5) and by high-resolution USGS lines (e.g., Fig. 4C; Johnson *et al.*, 1999).

At the northern end of the Seattle monocline, reflectors within the Blakeley Formation diverge in the southern end of the Seattle basin along an inferred wedge tip (Fig. 4A and B). At the northern end of the seismic line shown in Figure 4B, reflectors are monoclinally folded and uplifted above the divergent zone; below the divergent zone the reflectors are neither folded nor uplifted. (The Seattle monocline shown in Figure 4B is inferred from Figures 4C and 5, which image this structure much more clearly than does the line in Figure 4B.) Given the structural prominence of the Seattle monocline, we interpret this divergence (reflection inflection) as being structural rather than depositional.

We interpret the inflection as caused by the tip of a triangle zone (Fig. 3C) rather than by fault-propagation folding (Fig. 3A; Pratt *et al.*, 1997; Johnson *et al.*, 1999). In contrast to Pratt *et al.* (1997) we interpret the reflectors at the tip of the triangle zone to lie within the Oligocene and Upper Eocene Blakeley Formation rather than at the boundary of the Blakeley and the Blakely Harbor Formations (Fig. 4B). We interpret a package of faint, rhythmic, higher frequency north-dipping reflections within the triangle zone as originating from Tertiary sedimentary rocks (labeled Bl, Eocene sed. rocks, in Fig. 4B; and labeled B in Fig. 7) resting on top of the uplifted Eocene volcanic basement. The continuity of these layered reflectors as well as their seismic velocities of less than 4.5 km/s (ten Brink *et al.*, 2002) identifies them as Tertiary sedimentary rocks rather than Eocene volcanic rocks.

Determining the subsurface location of this inflection is critical for structural models because it corresponds to the location of the tip of the triangle zone (Fig. 3C). Using six high-resolution USGS seismic reflection profiles (Johnson *et al.*, 1999), we mapped the subsurface location of the tip (Fig. 4B) across the Puget Lowland (Table 1; Fig. 1). The tip was mapped as the location where the dip of the base of the Quaternary reflector identified by Johnson *et al.* (1999) changes subtly from southerly to northerly (e.g., Fig. 4B). The change in dip at the wedge tip is subtle because the leading edge of the wedge tip is very thin and does not require a large dip change in the overlying strata. Although small, this inflection is clearly recognizable in the SHIPS lines (Fig. 5). Our mapping of these inflection points defines a nearly linear wedge tip lying 1 to 3 km to the north of the surface "deformation front" mapped by Blakely *et al.* (2002).

Seismic Evidence for a Triangle Zone Along the Tacoma Fault Zone

As along the Seattle monocline, folded but unfaulted south-dipping reflectors along the Rosedale monocline (Johnson *et al.*, 2004) provide evidence for a triangle zone beneath the frontal portion of the Tacoma fault zone. The

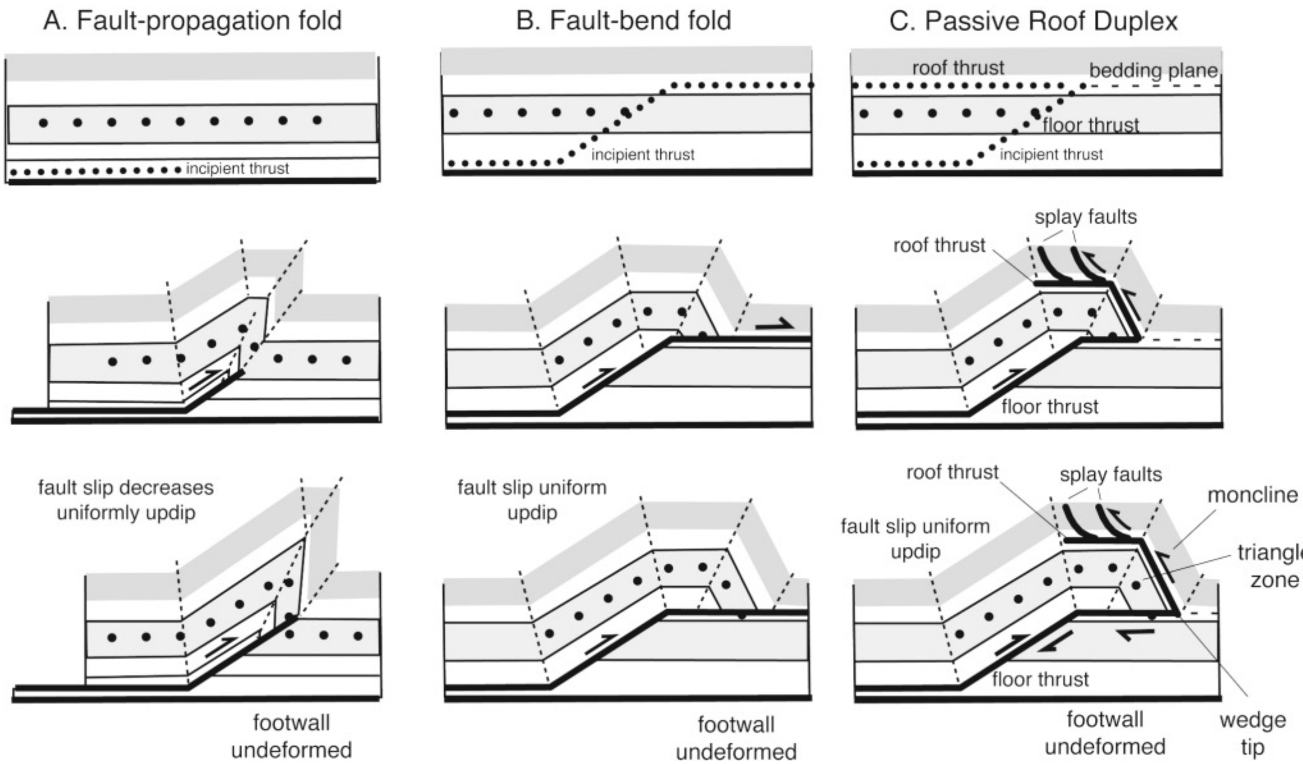

Figure 3. Illustration of (A) fault-propagation fold (Suppe and Medwedeff, 1990), (B) fault-bend fold (Suppe, 1983), and (C) passive-roof duplex (Jones, 1996b), defining structural terminology. Note that there is no requirement in a passive-roof duplex for a bedding plane thrust to exist in front of the wedge tip. Hence the dashed line at the right may represent either a bedding plane or a bedding-plane thrust.

Rosedale monocline is distinctly imaged in industry seismic lines (e.g., Fig. 4F).

Divergent reflectors within the sedimentary strata of the Tacoma basin between 2- and 2.5-sec twtt also provide support for a triangle zone along the Tacoma fault zone as imaged by oil industry lines (Fig. 4F). These migrated data reveal a deeper, subhorizontal to shallowly north-dipping event at about 2.5 sec that can be traced faintly across the entire section (and cannot be a multiple reflection since no overlying reflection has that sense of dip). These north-dipping reflections diverge from overlying south-dipping reflections associated with the Rosedale monocline above 2.5-sec twtt (Johnson *et al.*, 2004). (South-dipping reflections beneath this north-dipping reflector, not honored by our interpretation, presumably represent either interbed multiple reflections that could not be suppressed [because the data are single-fold] or reflections from sedimentary units within the tectonic wedge.) Divergent reflections cannot be explained by a step-up in a proposed 20-km-deep detachment surface (Pratt *et al.*, 1997; Johnson *et al.*, 2004). West of the Rosedale monocline we mapped the tip of the triangle zone along the Tacoma fault zone (Fig. 1) using the subsurface location where the dip of the Miocene and younger basin fill changes from northerly to southerly in USGS and industry lines.

Constraints on the Floor and Imbricate Thrust Geometry

Evidence for the floor and imbricate thrust geometry is less compelling than for the roof thrust geometry. One reason for this is that the wedge tips are not associated with potential field lineaments (Fig. 6) because they lie within the Seattle and Tacoma basins and have physical properties that do not differ significantly from surrounding rocks. Another reason is that both the hanging and floor walls of these faults often lie within the Eocene volcanic basement. We can, however, identify a reflection from the floor thrust of the Seattle fault zone as lying subparallel but slightly below the reflector identified by Pratt *et al.* (1997) in the Eocene volcanic basement (Figs. 4B and 7). Faint, south-dipping fault-plane reflections from a south-dipping imbricate thrust south of the Seattle fault zone abruptly truncate north-dipping reflections from inferred Tertiary sedimentary strata (labeled B in Fig. 7).

South of the Seattle fault's floor thrust, reflectors inferred to represent imbricate thrusts within the Eocene volcanic basement have a southerly dip of about 35° (Figs. 4B, 4D, 4E, and 7). These reflectors appear to project upward to offsets in the top of the Eocene volcanic basement. Owing to a gap in deep seismic reflection coverage south of Vashon

Island (Fig. 1), the lines image only the southern tip of the floor thrust beneath the triangle zone within the Tacoma fault zone (Fig. 4F).

Seismic Evidence for Shallow Thrusting and Folding Along the Seattle Uplift

Seismic lines along the Seattle uplift provide evidence for a series of shallow (upper 1- to 2-km) folds and splay thrusts. In this section we individually describe and discuss each of these shallow folds and thrusts.

Alki/Restoration Point Anticline. Pratt *et al.* (1997), Johnson *et al.* (1999), and Calvert *et al.* (2001, 2003) described seafloor deformation and uplift across the Alki/Restoration Point area (Fig. 4B) and interpreted several south-dipping faults in this location (e.g., Fig. 5). Seismic lines from this part of the Seattle uplift are challenging to interpret because of the shortage of continuous reflections, the steep 60°–90° dip of the strata (Yount and Gower, 1991), and the tight spacing of thrusting.

We interpret seismic lines and outcrops in the Alki/Restoration Point area as showing structural relief associated with shallow thrusting along closely spaced north-dipping thrusts (faults F1 to F5) (Fig. 4B). The five faults are inferred from undulations in the seafloor, from undulations in the inferred top of the Tertiary sedimentary strata, and from abrupt truncations of reflectors within these strata. Faults F1 to F3 are interpreted as high-angle faults, whereas F4 and F5 appear to have a moderate dip. From outcrops near Restoration Point (Yount and Gower, 1991), the dotted line in Figure 4B lies close to the boundary of the Oligocene and Upper Eocene Blakeley Formation and the Miocene Blakely Harbor Formation (Fig. 2). On Bainbridge Island this boundary is mapped as a fault (Waldron, 1962).

The Seattle monocline, having moderate (28°) northerly dips where best imaged by USGS lines P6 to P8 in Lake Washington (Fig. 4C) is also recognized in the SHIPS data (Fig. 5). From the geometry of the Seattle monocline, fault F1 (Fig. 4B) is inferred to lie along or subparallel to bedding planes. The location of fault F2, associated with a large bump on the seafloor, is consistent with the eastward projection of the Toe Jam Hill fault, an up-to-the north backthrust (Nelson *et al.*, 2002). The location of fault F3 (Fig. 4B), inferred mainly from a seafloor undulation but also from reflector termination (at a twtt of 0.95 sec), is consistent with the southeastward projection of the Waterman Point scarp, another up-to-the north backthrust (Nelson *et al.*, 2002; 2003a).

Fault F5 is defined by divergent and dipping reflections as well as by potential fault-plane reflections (Fig. 4B). It is interpreted as a bedding plane thrust. The internal structure of the Tertiary sedimentary rocks between faults F1 and F4 are not well imaged in available reflection data (e.g., Fig. 4B), possibly because of the steep dips revealed in nearby outcrop (Yount and Gower, 1991), and hence the geometry of these faults is poorly constrained.

Blake Island Anticline. The Blake Island anticline, informally named here after the small island lying to the north of the anticline, was first mapped as anticline A by Pratt *et al.* (1997) (Fig. 4B). Folded reflectors defining a relatively open anticline about 3 km wide are imaged in industry and SHIPS seismic lines (Fig. 4B). The dashed line likely highlights a horizon within the Oligocene and Eocene sedimentary strata, because no Miocene sedimentary strata are mapped south of Alki Point (Yount and Gower, 1991).

We interpret the Blake Island anticline as truncated to the south by a north-dipping thrust (F6) splaying up from a shallow roof thrust. The longest limb of the Blake Island anticline dips to the north, consistent with a north-dipping thrust (F6). Some reflectors appear to continue across the inferred fault (F6), but the abrupt decrease in reflection amplitudes across F6 suggests to us that this continuity is only apparent (Fig. 4B). Late Quaternary growth for this anticline is inferred from relief of the Quaternary/Tertiary unconformity, although the growth rate is slow as the seafloor does not exhibit evidence of folding.

Winghaven Park Anticline. The Winghaven Park anticline, informally named here after a park on its projection, is imaged as a broad (2.5-km-wide) fold located south of a broad (2-km-wide), low-amplitude syncline (Fig. 4D). Reflections define an asymmetric anticline that locally steepens to the north. Abrupt truncation of these reflections to the south suggests a short, north-dipping backthrust (fault F7). Quaternary growth of this anticline is indicated by gently north-dipping reflections from the base of Quaternary deposits overlying it.

Seahurst Park Anticline. The Seahurst Park anticline, informally named here after a park at the same latitude, is a narrow (1-km-wide), asymmetric fold having a long, north-dipping backlimb (Fig. 4D). The fold is imaged both within the Tertiary sedimentary strata and along the contact between the Tertiary and the Quaternary deposits. Its narrow, kinked geometry requires very shallow thrusting. The extreme asymmetry of the fold requires a north-dipping fault bounding its southern flank (fault F8). Late Quaternary growth on this anticline is suggested by its shallow depth of burial beneath the seafloor. A low growth rate is inferred from the undeformed, subhorizontal seafloor above it.

South of the Seahurst Park anticline, minor offsets of inferred Tertiary horizons and the Quaternary/Tertiary unconformity provide evidence for faults F9 and F10 (Fig. 4D). Although we interpret these structures as north-dipping faults, the direction of dip is poorly constrained. The southward shoaling of reflectors inferred to represent Tertiary sedimentary strata suggests that the roof thrust, thought to lie at the top of the Crescent Formation (see subsequent discussion entitled Depth to Top of Eocene Volcanic Basement), also shoals southward from the Seahurst Park anticline. The seafloor above these faults is not offset, but the short depth interval between the seafloor and the Quaternary/Tertiary unconformity suggests that deformation above the faults approaches the seafloor. Thus, these relations suggest

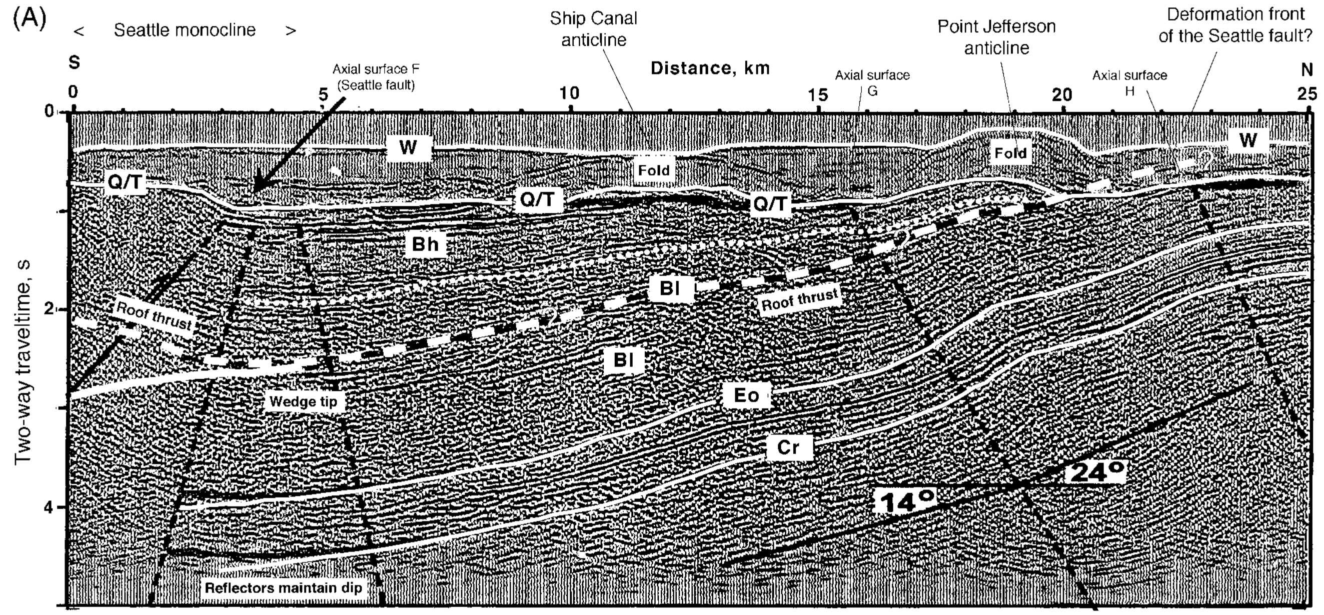

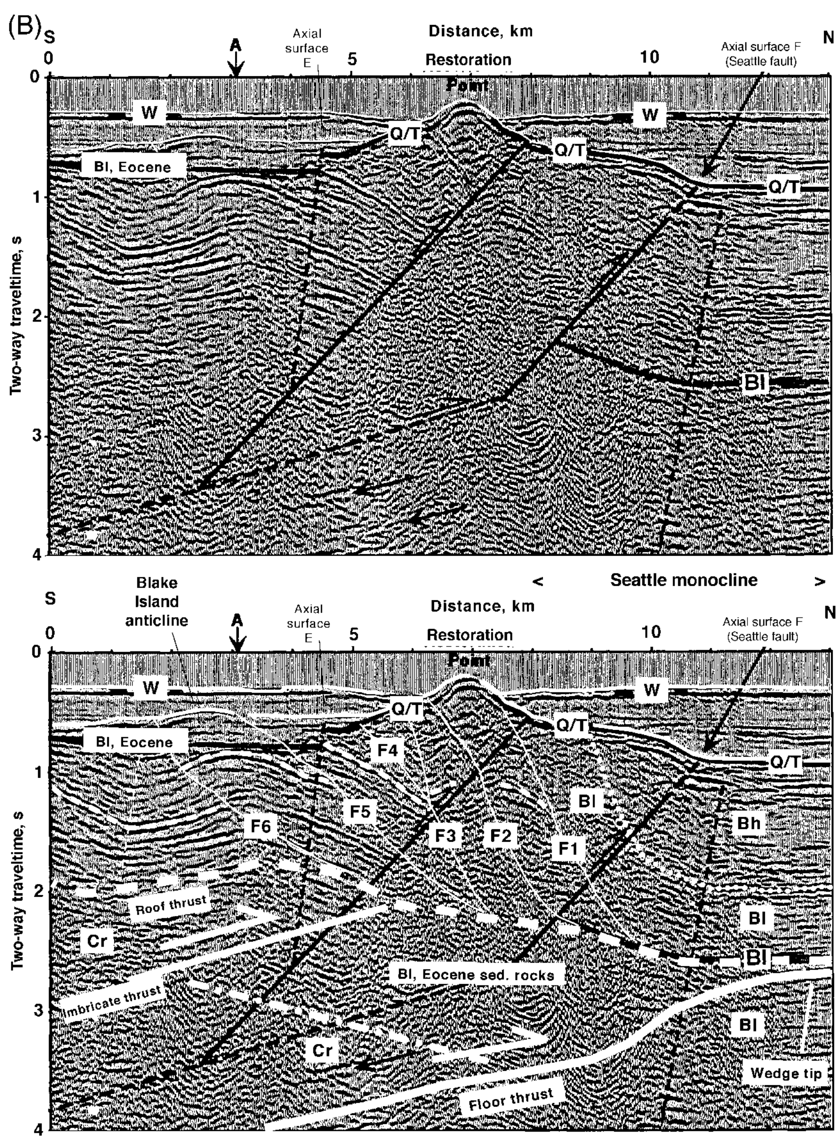

Figure 4. Interpretation of industry and USGS seismic reflection lines. (A) Migrated seismic line over the Seattle basin (modified from Pratt *et al.*, 1997). (B) Seattle fault zone as interpreted by Pratt *et al.* (1997), (top) and our interpretation, (bottom). (C) Migrated, six-fold seismic line over the Seattle monocline imaged in Lake Washington (modified from Johnson *et al.*, 1999). (D) Line drawing interpretation of seismic line over the northern Seattle uplift. (E) Line drawing interpretation of seismic line over the southern Seattle uplift. (F) Migrated single-fold seismic line over the Rosedale monocline near Tacoma (modified from Pratt *et al.*, 1997). In Figure 4B, the geometry of the Seattle monocline is inferred from Figure 5. The thin white line highlights the seafloor reflector (shown as a gray line for D and E), thinner white lines highlight splay thrusts that sole into a roof thrust, the dashed thick white line highlights inferred roof thrust, and the thick solid white lines show the location of floor and imbricate thrusts. Dotted, dashed, and dash-dot white lines highlight reflectors within Tertiary sedimentary rocks in the Seattle basin, Seattle uplift, and Tacoma basin, respectively (wish the ages of these reflectors varying at each of these three locations). The bases of Quaternary deposits and the tops of the Tertiary sedimentary rocks are shown as a thin white line (and as a gray line in D and E). Black solid and dashed lines show prior interpretations of Pratt *et al.* (1997) and Johnson *et al.* (1999). Abbreviations: W, base of seawater; Hol., Holocene; Q/T, Quaternary/Tertiary unconformity; Bh, Blakely Harbor Formation; Bl, Blakeley Formation; Eo, Eocene sedimentary rocks; Ol, Oligocene sedimentary rocks; Cr, Crescent Formation. (*continued*)

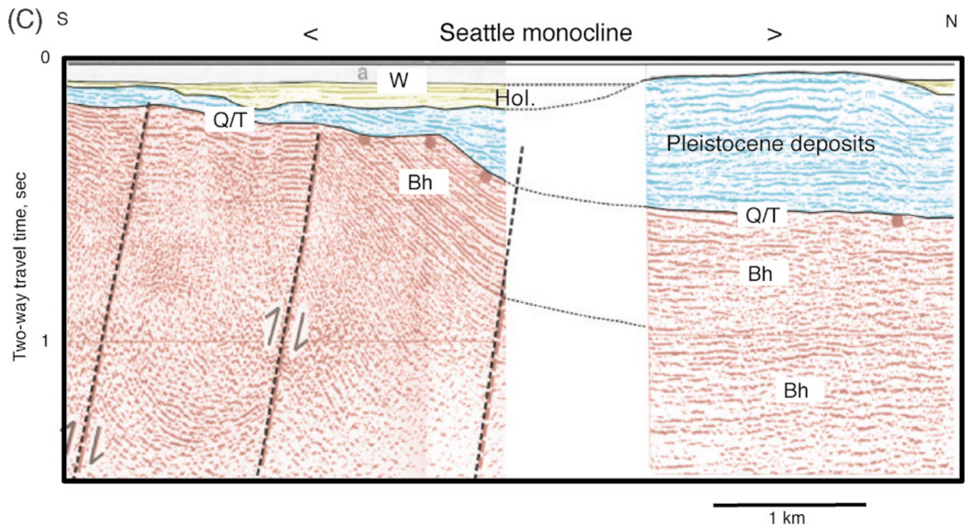

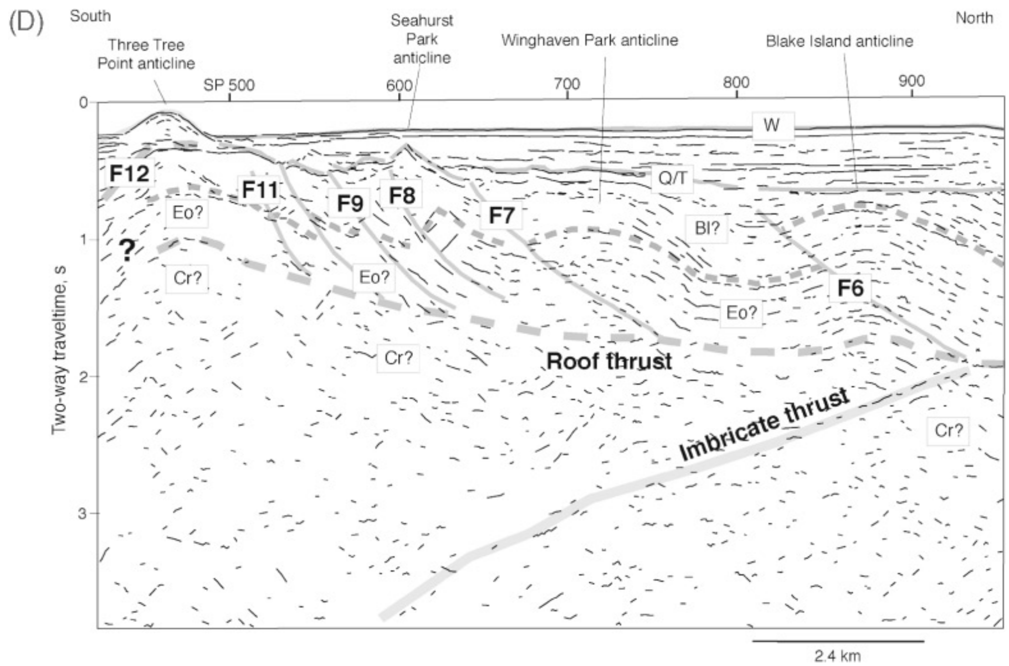

Figure 4. *Continued.*

higher rates of late Quaternary growth than observed for the Blake Island and Winghaven Park anticlines.

Three Tree Point Anticline. Along the westward projection of Three Tree Point the seafloor reflection arches upward and stands about 0.2 sec twtt (150 m) higher than the surrounding seafloor (Fig. 4D and E). Reflections from Tertiary units to the south of Three Tree Point arch upward toward the north very close to the surface, suggesting that the seafloor arch has a structural rather than a glacial origin. Consistent with this interpretation, reflectors from Tertiary sedimentary strata to the north define a deeper anticline with a north limb about 1.5 km wide beneath Three Tree Point.

Available seismic lines do not unambiguously define the sense of dip of this shallow faulting. We interpret the flat shallow reflection as evidence for a north-directed thrust fault rather than erosional beveling of the anticline, but we allow that interpretations of south-directed thrusting from these seismic data are possible. In any case, the fold relations suggest late Quaternary growth of this structure.

Relief of the arch is related, in our interpretation, to structural repetition caused by both north- and south-directed thrusting. Thrust fault F12 must dip southward because the longest fold limb above it dips southward (Fig. 4E). In our interpretation, north-directed thrusting along

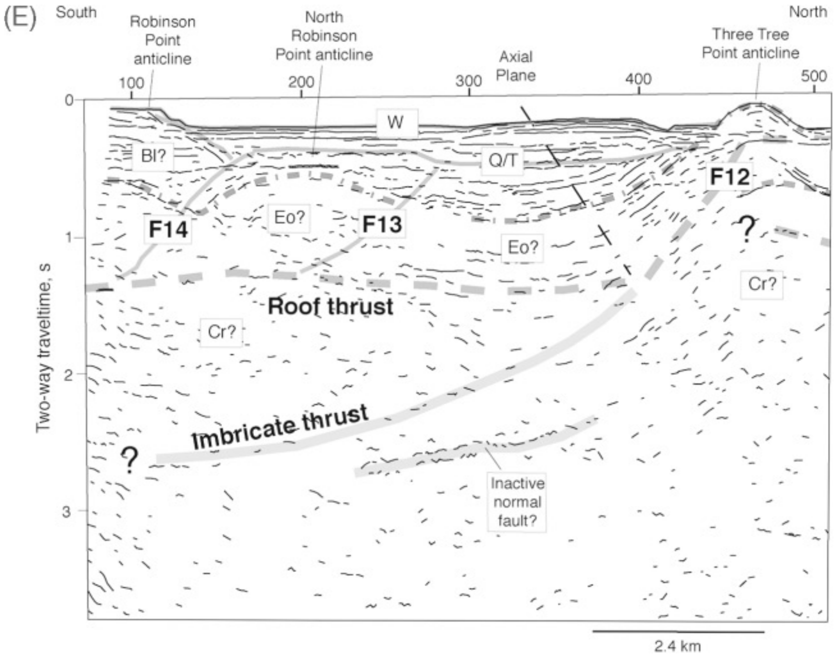

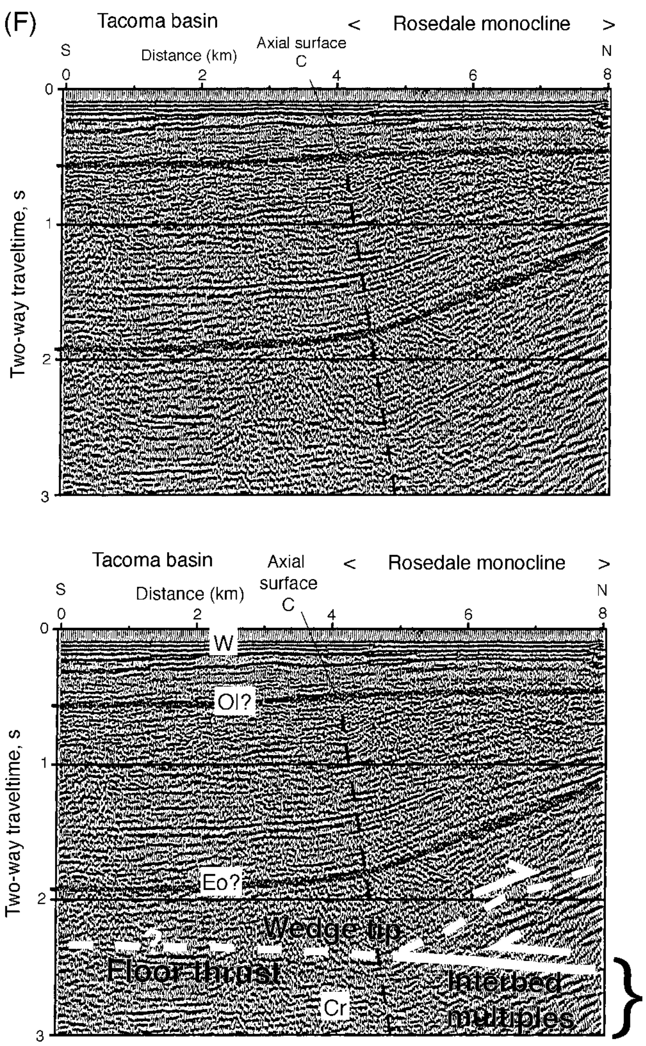

Figure 4. *Continued.*

fault F12 overrides and overlaps the south-directed roof thrust system into which faults F8, F9, F10, and F11 root. The fold above fault F12 may originate from either imbricate thrusting or a bend in a roof thrust located just to the south of the Three Tree Point anticline. A broad (3-km-wide), low-amplitude syncline south of the Three Tree Point anticline is interpreted as related to a minor depression in the roof thrust below it, perhaps associated with earlier offset on an inactive structure within the Crescent Formation. We interpret F12 as a shoaling of the roof thrust system extending northward from the Tacoma fault zone. In Figure 4E, south of the Three Tree Point anticline, the line pattern changes from dashed to dash-dot for reflections within the Tertiary sedimentary rocks reflecting our uncertainty of the age of the reflectors in the Tacoma basin, where deep boreholes and outcrops of Tertiary sedimentary rocks are both absent. Although the dashed and dash-dot reflectors may both represent Tertiary sedimentary rocks of comparable ages, we currently lack evidence that this is the case.

Point Robinson North Anticline. A few kilometers north of Point Robinson, reflectors show a broad (2-km-wide) anticline with an axis at SP 200 (Fig. 4E). We refer to this anticline informally as the Point Robinson North anticline, to distinguish it from the Point Robinson anticline to the south described in the next section. Its longer south-dipping backlimb requires a south-dipping fault (F13). Fault F13 may produce the observed flat-lying reflections at 1.3 to 1.4 sec twtt. Fault F13, however, is not defined by reflector truncation; indeed, the reflectors seem continuous but are abruptly bent across it, perhaps by a fault-bend fold. Fault F13 deforms the base of the Quaternary as drawn (Fig. 4E). Seafloor topography between Three Tree Point and Point

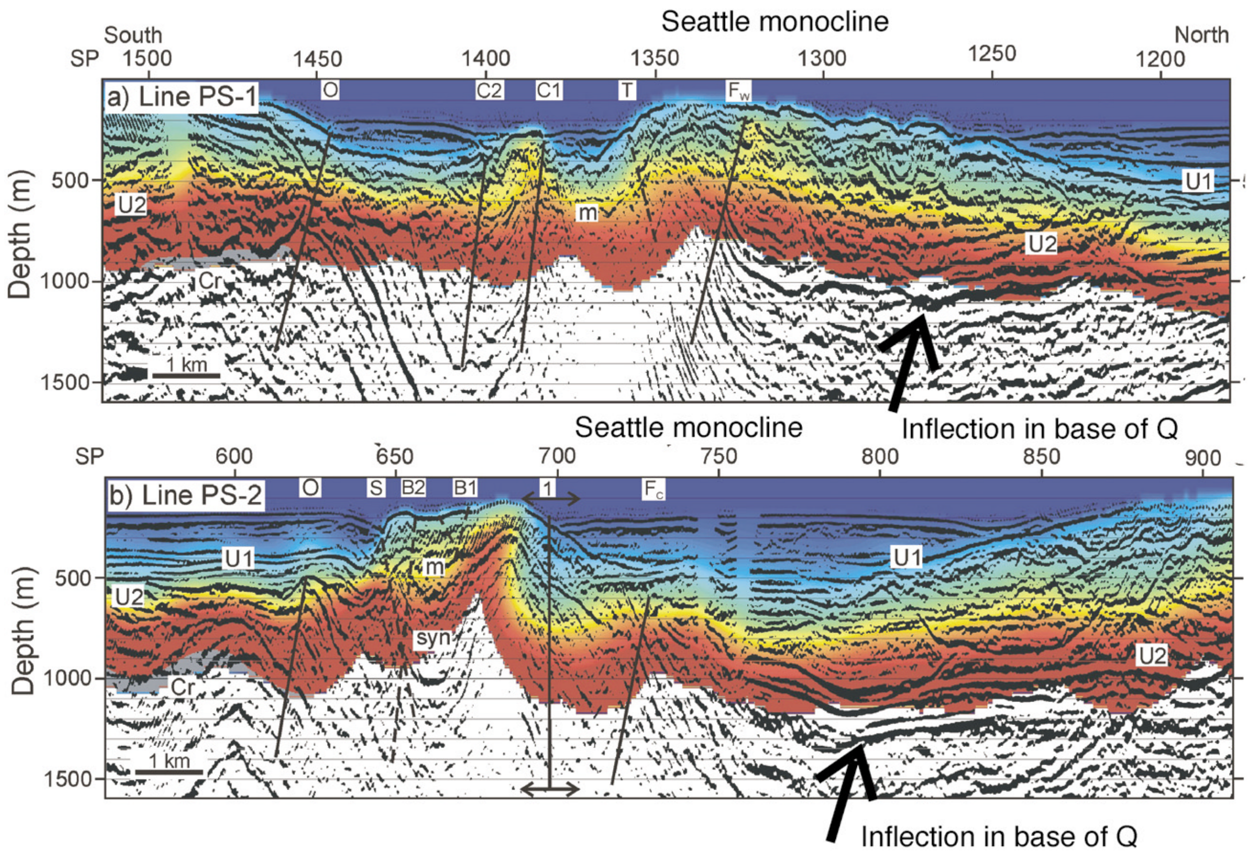

Figure 5. Illustration of the inflection in the Quaternary/Tertiary unconformity (labeled U2) imaged by the SHIPS seismic reflection data, providing information on the location of the inferred wedge tip (modified from Calvert *et al.*, 2003). Labels O, S, B2, B1, 1, C2, C1, T, F_w, and F_c refer to mainly south-dipping faults interpreted by Calvert *et al.* (2003). Abbreviations: Cr, Crescent Formation; m, multiple; syn, syncline; U1, Holocene/Pleistocene unconformity.

Table 1
Inflection Points Along the Seattle Fault Zone from Profiles in Johnson *et al.* (1999)

Line	Location	Distance (in km) of Inflection from North End of Published Line
5A	Lake Washington	0.8
5B	Elliot Bay	0.9
5C	Eastern Puget Sound	1.3
5D	Central Puget Sound	3.8
5E	Western Puget Sound	Not imaged
5F	Port Orchard	0.25
5G	Dyes Inlet	0.1

Robinson (SP 100 on the industry line) is subdued, however, indicating that the Point Robinson North anticline and fault F13 had less Quaternary growth and slip than either the Point Robinson or Three Tree Point anticlines.

Robinson Point Anticline. This eastward-trending anticline located a few kilometers southeast of Point Robinson (Fig. 1) was first recognized by Pratt *et al.* (1997). Reflectors on industry and SHIPS seismic lines image seafloor uplift over the anticline (Fig. 4E). The seafloor uplift overlies arched reflectors in Tertiary sedimentary strata favoring a structural rather than depositional origin. The fold is a broad (3-km-wide), asymmetric anticline with a longer south-dipping backlimb (not shown) requiring a south-dipping, north-vergent fault (F14). Fault F14 abruptly truncates north-tilted strata on the northern end of the anticline (Fig. 4E). Late Quaternary growth of the anticline is inferred from the arching of the seafloor along it.

Depth to Top of Eocene Volcanic Basement

Relief on the top of the Eocene volcanic basement along the Seattle uplift and in the adjacent Tacoma and Seattle basins provides a measure of the vertical deformation associated with the uplift. A wide variety of geologic and geophysical data suggest that Eocene volcanic basement rocks are either shallow or crop out along the uplift. This evidence includes (1) outcrops of Eocene basalts (Fig. 1) to the east and west of Puget Sound (Waldron, 1962; Haeussler and Clark, 2000), (2) penetration of these volcanic rocks on the southwestern end of the uplift at a depth of 95 m below sea

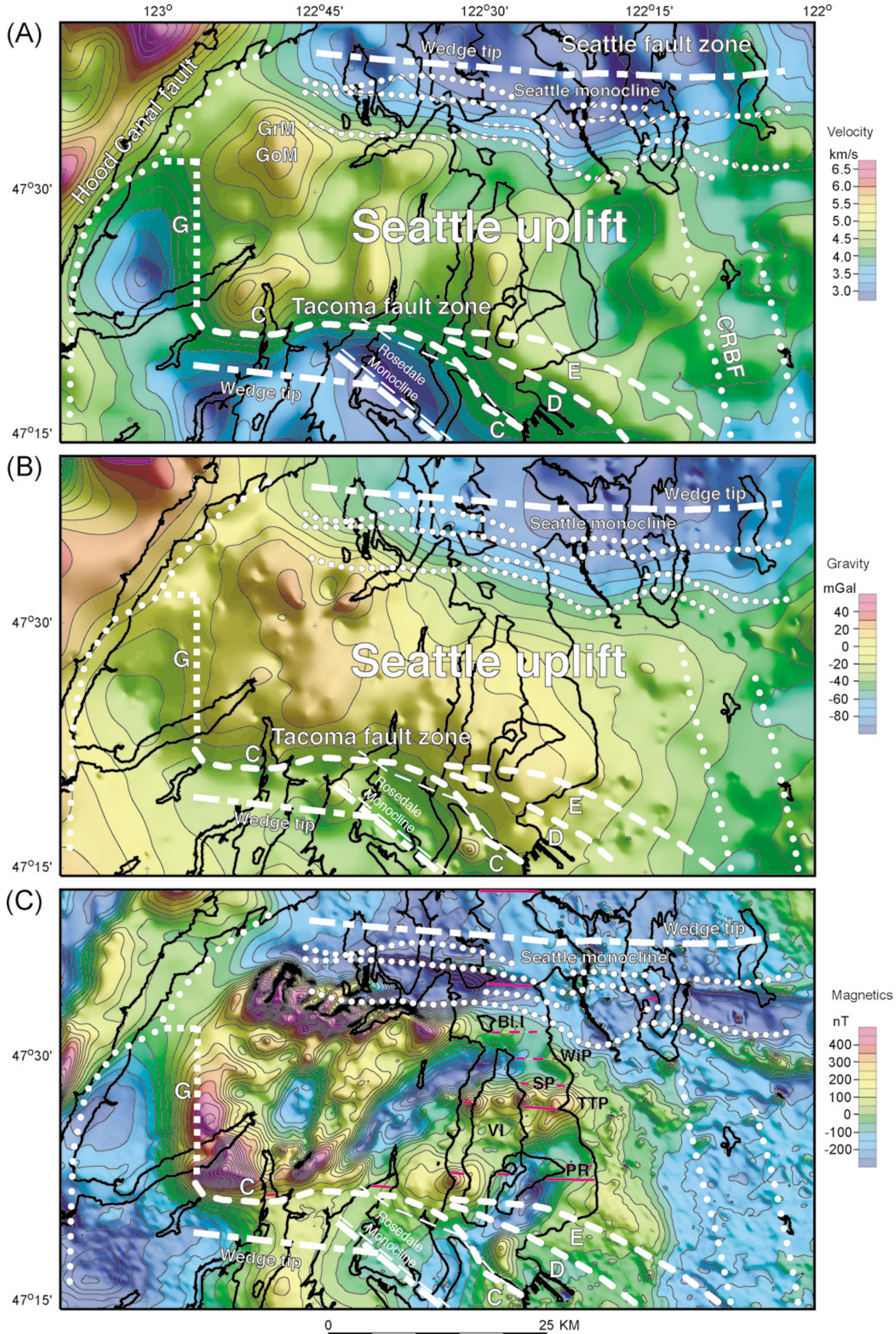

Figure 6. (A) Seismic velocity model from SHIPS tomography at 3 km (Brocher *et al.*, 2001), (B) isostatic gravity anomaly, and (C) aeromagnetic anomaly maps of the Seattle uplift. Locations of wedge tips and the Rosedale monocline (Johnson *et al.*, 2004) mapped from the seismic lines are superimposed on these anomalies (as dashed and dotted lines). Dotted lines show locations of inferred or known crustal faults. Dashed lines (labeled C, D, E, and G) identify lineaments defined by the geophysical data. Abbreviations as in Figure 1. Magenta lines in Figure 6C show the locations of the anticlinal crests as mapped in Figure 1.

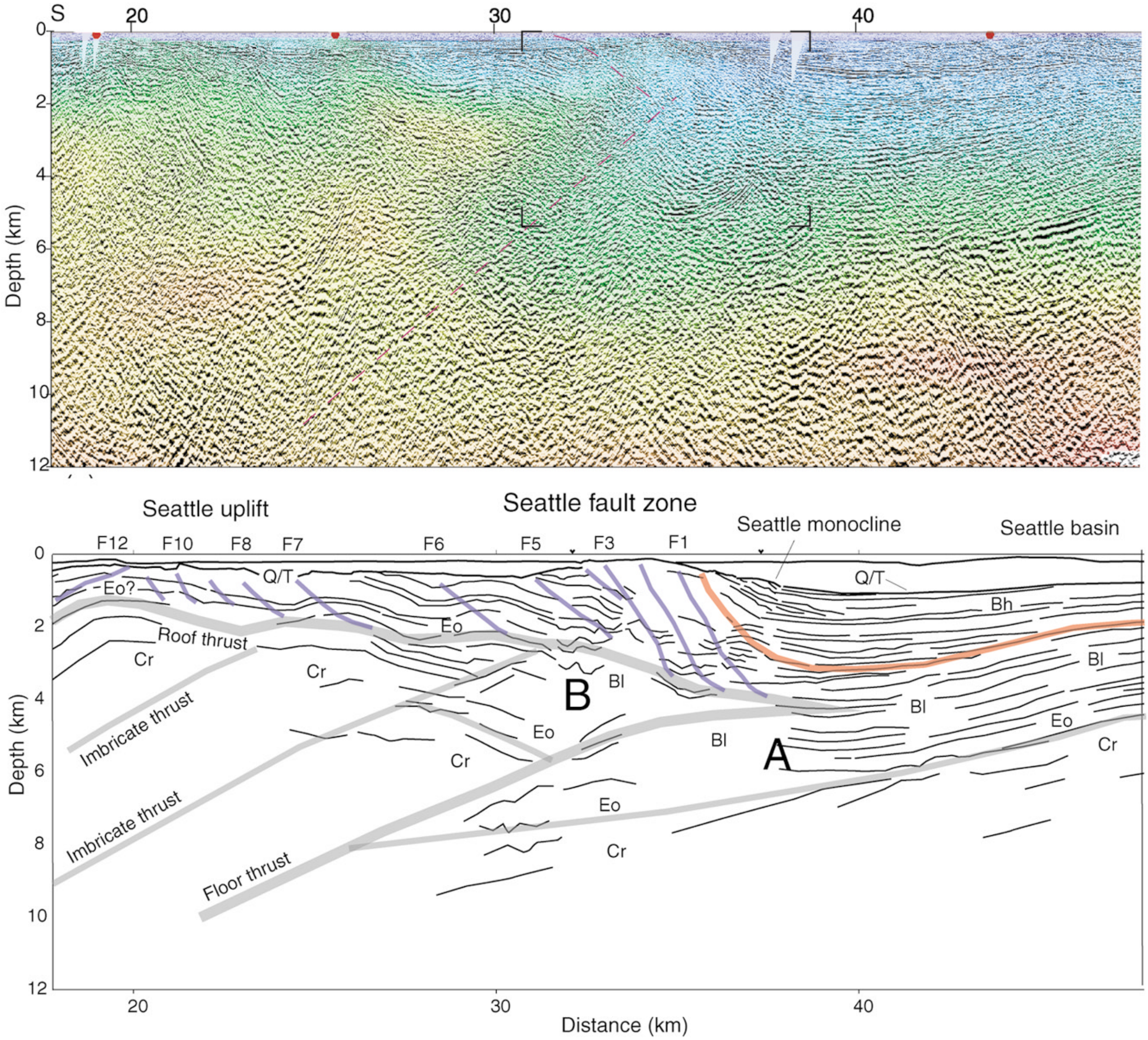

Figure 7. (Top) A portion of SHIPS seismic reflection line PS-2 and coincident P-wave velocity model in Puget Sound (modified from ten Brink *et al.*, 2002). Seismic line is time migrated and depth converted. Colors superimposed on line present a SHIPS tomography velocity model (see ten Brink *et al.*, 2002). (Bottom) Line drawing interpretation of these reflection data by ten Brink *et al.* (2002), over which we have transposed our interpretation of the top of Crescent volcanic basement (Cr), and the splay, roof, imbricate, and floor thrusts along the Seattle fault zone. Shallow splay faults F1 to F12 that root into the roof thrust (blue lines) and the base of the Miocene Blakely Harbor Formation (orange line) are also identified. Reflections labeled A are interpreted as overmigrated reflections within the Blakeley Formation. North-dipping reflectors labeled B are interpreted as reflections from the Blakeley Formation and Eocene sedimentary strata. Abbreviations as in Figure 4.

level in the Hofert #1 industry well (Sceva, 1957), (3) high-amplitude gravity, magnetic, and tomographic anomalies characteristic of this formation over the eastern and western ends of the uplift (Fig. 6), and (4) a lack of coherent reflectivity below the roof thrust south of the Blake Island anticline at shallow depths (Fig. 4D and E) of 1.2 to 2.2 km, inferred from seismic reflection travel times of 1 and 1.5 sec twtt (Brocher and Ruebel, 1998). These latter depth estimates are for test holes on the Kingston Arch most likely representative of the Oligocene and Eocene strata overlying the Seattle uplift. If the Seattle uplift is instead underlain by the Eocene Puget Group (Fig. 2), as at the Washington State #1 and Blessing Siler Community #1 wells, a 10%–20% greater depth would be inferred (Brocher and Ruebel, 1998).

A shallow depth to the top of Eocene volcanic rocks is also consistent with seismic tomography and gravity data (Fig. 6). Seismic velocities of 4.5 km/s and higher are correlated to Eocene volcanic rocks at the Mobil-Kingston #1 well (Snelson, 2001) on the Kingston Arch (Fig. 1). We therefore use the 4.5 km/s isocontour as a proxy for the top of the Eocene volcanic rocks (Fig. 8C), similar to the 4 to 4.5 km/s range used by ten Brink *et al.* (2002) for the top of basement. The depths inferred from this assumption correspond closely to the lower depth limit of stratified reflectivity along the Seattle uplift. Our definition may locally overestimate the depth to the top of the Eocene volcanic rocks, given that upper members of this formation commonly contain lower velocity sedimentary interbeds that could produce seismic reflections (Johnson *et al.*, 1994). However, our preferred geometry for the top of Eocene volcanic rocks provides a satisfactory fit to the gravity and magnetic data (Fig. 8A) and is similar to the magnetic model of Blakely *et al.* (2002).

To the north of the uplift, beneath the Seattle monocline and Seattle fault zone, we trace faint, discontinuous, south-dipping, deep reflections defining the top of the Eocene volcanic rocks beneath the triangle zone almost as far south as Winghaven Park, to a depth of about 8 km (Fig. 7). Partly based on their proximity to the 4.5 km/s isovelocity contour (Fig. 8C), we infer that these stratified reflections represent Tertiary sedimentary rocks and that their base corresponds to the top of the Eocene volcanic rocks.

Seismic Evidence for Deformation in the Seattle Basin

In our view the industry seismic lines provide permissive evidence that the northward propagation of the Seattle fault zone is deforming the Seattle basin. This view is based on a new interpretation of two shallow, low-amplitude, short-wavelength sets of arched reflections imaged in the shallow section of the Seattle basin (Fig. 4A) (better displayed on a seismic profile shown in figure 2B of Johnson *et al.* [1994]). The prevailing interpretation of these arched reflections is that they represent velocity artifacts caused by mounds having a depositional—most likely glacial—origin (Johnson *et al.*, 1994; Pratt *et al.*, 1997). In this view, velocity contrasts developed between hills containing higher velocity glacial advance facies (e.g., till) and intervening lower velocity uncompacted recessional outwash/Holocene strata could generate velocity artifacts that mimic folding.

As an alternative model, we suggest that these arched reflections could represent fault-bend folds (Fig. 4A) because they directly overlie folds in underlying strata. In this model the arches are folds reflecting slip and step-ups along this curved bedding plane thrust within the Blakeley Formation. The inferred bedding plane thrust would stretch northward from the wedge tip of the Seattle fault to the south limb of the Kingston Arch (Fig. 4A). Slip along the contact between the Crescent Formation volcanic rocks and the base of the Tertiary sedimentary rocks may also explain this folding, as implied by the hypocenter and focal mechanism of the 1997 Bremerton earthquake (Dewberry and Crosson, 1996), discussed in a following section. The larger amplitude of these shallow folds compared to those of folds in underlying strata is only apparent and results from the display in terms of travel time rather than depth. In our view the underlying folds cannot simply represent artifacts resulting from velocity pull up, because their geometry is not well correlated to the geometry of the seafloor.

We emphasize that the proposed folding in the Seattle basin is not a requirement of the passive-roof duplex models, but we note that deformation within molasses basins associated with basin-bounding thrust faulting (Fig. 9) is commonly observed (Banks and Warburton, 1986). We informally name the southernmost of these proposed folds, located at the latitude of the Seattle Ship Canal, as the Ship Canal anticline. We informally name the northernmost proposed anticline the Point Jefferson anticline for its location just south of Point Jefferson on Kitsap Peninsula (Fig. 1).

Other Evidence for Shallow Folding and Thrusting

Deformation of the Seattle Basin

Water wells intersecting the top of Tertiary sedimentary rocks generally lie along a narrow belt located along the major folds in the Alki/Restoration Point areas (Sceva, 1957; Yount and Gower, 1985; Jones, 1996a). Exceptions to this rule are wells lying along the projections of anticlines having late Quaternary growth, as mapped in the seismic profiles (Fig. 1).

Consistent with a structural origin for the Seattle Ship Canal anticline, water wells on both sides of Puget Sound intersect Tertiary sedimentary units along its projection (Fig. 1). A well along the Seattle Ship Canal reached Tertiary units about 174 m below sea level, whereas wells of comparable or greater depth to the north and south did not (Yount and Gower, 1991). West of the Sound, a well on Bainbridge Island in Battle Point Park (Fig. 1) intersected probable Tertiary sedimentary units above 230 m below sea level (Sceva, 1957).

Evidence for Shallow Thrusts Beneath the Seattle Uplift

Shallow splay thrusting along the Seattle uplift, having a ramp and flat pattern, is inferred from the shallow down-dip termination of shallow thrusts and from the short wavelength of shallow folds and thrusts. These characteristics are best exhibited by the Winghaven Park and Seahurst Park anticlines and faults F7 and F8 (Fig. 4D).

Our interpretation of the roof thrust as a bedding plane thrust is consistent with the nearly constant stratigraphic thickness between it and inferred Oligocene/upper Eocene reflectors (dashed and dash-dot lines in Fig. 4B, D, and E). Thrusting along bedding planes is also indicated by the parallelism of long fold backlimbs along the inferred roof thrust. North-side-up thrusting along steeply dipping bedding

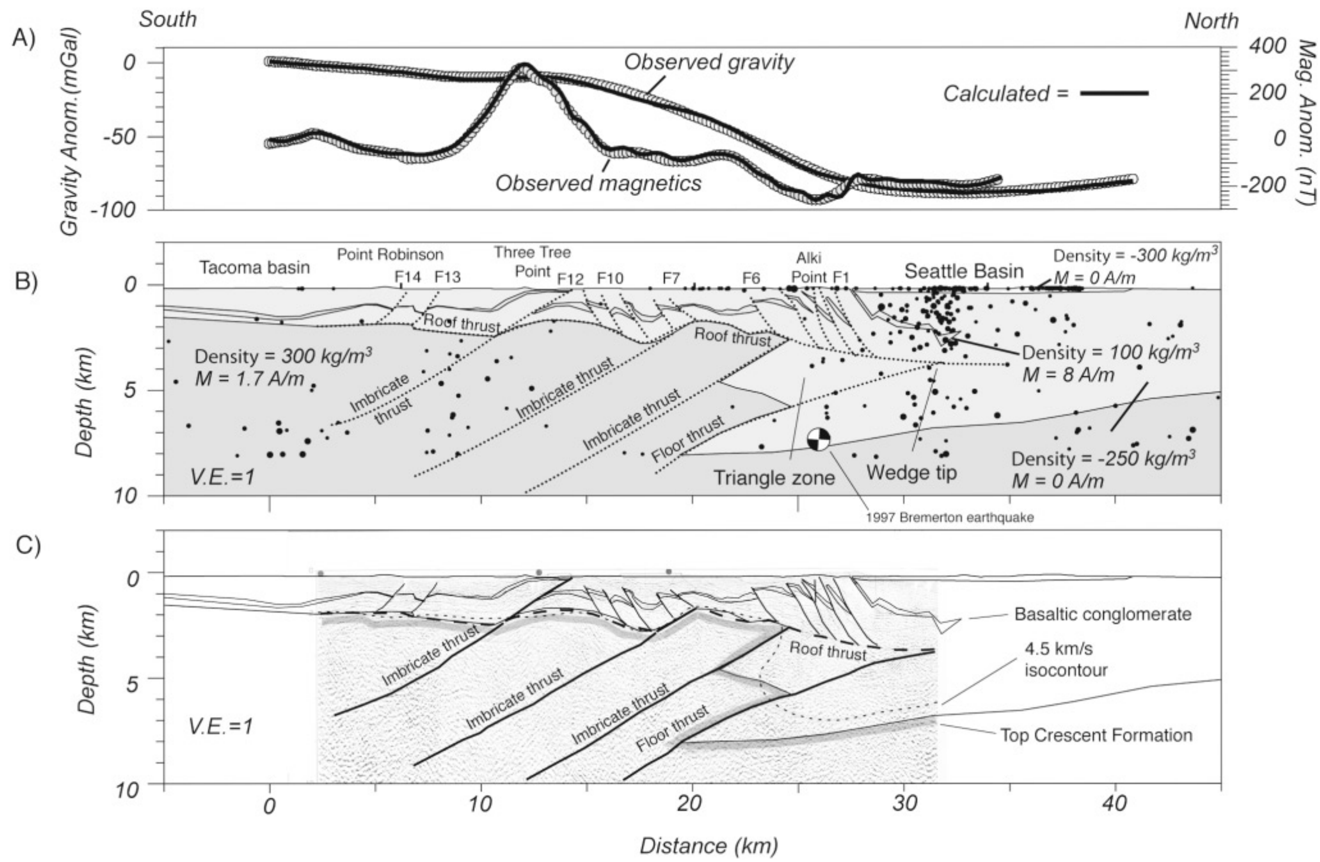

Figure 8. (A) Comparison of observed and calculated magnetic and gravity profiles along Puget Sound. (B) Magnetic and density models used to calculate anomalies in Figure 8A. (C) Interpreted migrated, depth-converted SHIPS line PS-2 across the Seattle uplift, modified from ten Brink *et al.* (2002). Thick gray line, top of the Eocene volcanic basement; dotted line, 4.5 km/s isocontour; polygons, basaltic conglomerate unit. Seismicity plotted in the upper 8 km was recorded from 1972 to 2003, for the box shown in Figure 11. Earthquakes were projected eastward and westward onto the cross section in Figure 8B. Focal mechanism for the 1997 Bremerton earthquake (Blakely *et al.*, 2002) is superimposed.

planes in fault-scarp excavations along the Toe Jam Hill and Waterman Point strands of the Seattle fault zone at Bainbridge Island (Nelson *et al.*, 2002, 2003a,b) provide strong support for this interpretation.

Near Restoration and Alki Points, strata in the Blakely Harbor and Blakeley Formations dip steeply northward between 60° and 90°, with an average dip between 70° and 75° (Yount and Gower, 1991). These steep dips are consistent with our interpretation of thrusting along steeply dipping splay faults F1 to F5 (Fig. 7).

An inferred roof thrust originates at the tip of the triangle zone at the northern end of the Seattle uplift, where it follows the base of the Seattle monocline and the uppermost of the divergent reflections within the Blakeley Formation. Because of the low quality of available seismic lines there, a roof thrust can only be projected beneath Alki/Restoration Point (Figs. 4B and 7). South of Alki Point, however, the quality of the lines improves substantially and they define the roof thrust as the top of the Eocene volcanic rocks as far south as Point Robinson (Fig. 4B, D, and E). Between Point Robinson and the wedge tip south of Tacoma, a roof thrust is inferred to underlie the Rosedale monocline (Fig. 4F).

Borehole Evidence for Shallow Folding over the Seattle Uplift

An eastward-trending anticline in Eocene volcanic rocks in the Blue Hills (Gold Mountain) at the southern end of Sinclair Inlet mapped by Yount and Gower (1991) projects eastward toward the Blake Island anticline (Fig. 1). Several water wells at this latitude, south of Bremerton, intersect likely Tertiary sedimentary rocks above about 300 m below sea level (Sceva, 1957).

Along the Three Tree Point anticline two wells intersected Tertiary sedimentary units at shallow depth (Buchanan-Banks and Collins, 1994). These wells (numbers 18 and 19; Buchanan-Banks and Collins, 1994) intersect Tertiary sedimentary strata at 103 m and 75 m below sea level, respectively. A few kilometers to the east of these

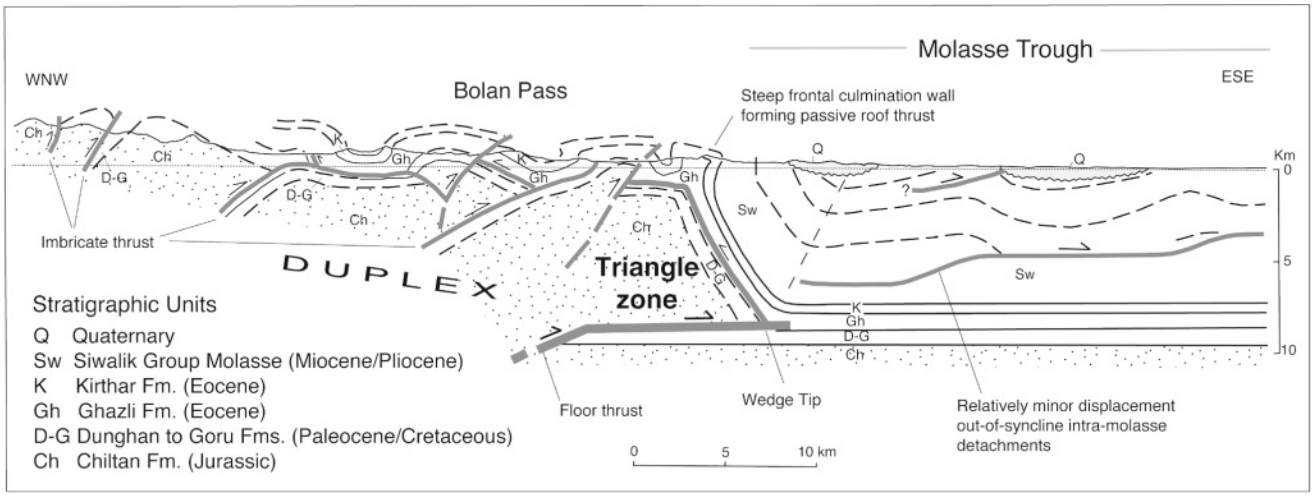

Figure 9. Passive roof duplex in Kirthar thrust belt at the Bolan Pass in Pakistan (modified from Banks and Warburton, 1986). Imbrication and shortening results in about 9 km of structural relief on the Jurassic formation (Ch) above its regional level. Note the formation of detachment faults in the foreland molasse basin.

wells (Fig. 1), Tertiary sedimentary strata and Eocene volcanic units crop out (Waldron, 1962).

Along the Point Robinson anticline, two wells intersected Tertiary sedimentary strata and Eocene volcanic rocks at shallow depths. West of Puget Sound, the Hofert #1 well (Fig. 1) intersected Eocene volcanic rocks at 95 m below sea level (Sceva, 1957). On the eastern shore of Puget Sound, Tertiary sedimentary units (bedrock?) were intersected 252 m below sea level by well number 57 of Buchanan-Banks and Collins (1994).

Aeromagnetic Anomaly Evidence for Shallow Folding over the Seattle Uplift

Prominent, short-wavelength aeromagnetic anomalies along the central part of the Seattle uplift coincide with the crests of shallow anticlines mapped by seismic lines in Puget Sound (Fig. 6C). This correlation allows the lengths of the anticlines to be estimated from the length of the magnetic anomalies. The Blake Island anticline forms the southern boundary of a prominent eastward-trending aeromagnetic anomaly. The anomaly amplitude is largest on its western end over the Blue Hills and progressively decreases in amplitude eastward, becoming difficult to trace east of Puget Sound. The aeromagnetic anomaly along the Blake Island anticline is approximately 40 km long; along much of its western end the anomaly must originate within the Eocene volcanic basement as there are few Tertiary sedimentary rocks in this location.

Three Tree Point anticline coincides with a prominent eastward-trending aeromagnetic anomaly about 15 km long (Fig. 6C). This anomaly, the most prominent of the short-wavelength anomalies along the entire profile (Fig. 8), is best developed between the Kitsap Peninsula and Three Tree Point.

The Point Robinson anticline is coincident with a discontinuous aeromagnetic anomaly that can only be traced on and west of Vashon Island. SHIPS line PS-1 west of Vashon Island and USGS line 316 from Quartermaster Harbor (between Vashon and Maury Islands) (Johnson *et al.*, 2004) image gently folded reflections and a deformed and uplifted seafloor. Johnson *et al.* (2004) inferred a high-angle fault in this location, as well as farther west in Case and Carr Inlets, that they named the Tacoma fault (Fig. 1).

Crustal models of the Seattle uplift and Seattle fault based on magnetic profiles along the Puget Sound have relied on two important magnetic rocks exposed in the area: basalts of the Eocene Crescent Formation and a volcanic conglomerate layer within the Miocene Blakely Harbor Formation (Blakely *et al.*, 2002; Hagstrum *et al.*, 2002). The high-amplitude magnetic anomalies discussed here have been accounted for in these models in various ways: Blakely *et al.* (2002) assumed that south-dipping reverse faults in the Crescent Formation generated the large magnetic anomalies of the Seattle uplift, whereas Hagstrum *et al.* (2002) assumed that dipping layers of reversely polarized Crescent Formation were important contributors. In both of these studies, the volcanic conglomerate was included only where exposed, near Restoration Point on Bainbridge Island.

Here we propose that shallow folding and truncation of this and similar older basaltic conglomerates, as well as vertical offset and folding of the Eocene volcanic rocks along imbricate thrusts, account for the short-wavelength aeromagnetic anomalies throughout the Seattle uplift. To test this hypothesis the depth and thicknesses of basaltic conglomerates and vertical offsets of the Eocene volcanic rocks inferred from the seismic lines were used to model the observed magnetic anomalies. The resulting magnetic model adequately predicts the large amplitude of the aeromagnetic anomaly over the Three Tree Point anticline as well as the more subdued anomalies along the remainder of the section (Fig. 8). We conclude that shallow folding and thrusting could explain these magnetic anomalies if suitably magnetic volcanic conglomerates and sufficiently large vertical offsets and folding of the Eocene volcanic rocks are present.

Geologic mapping provides evidence for the widespread deposition of basaltic conglomerates across the Seattle uplift. Volcanic conglomerates are mapped within the Eocene Tukwila Formation (Fig. 2), east of Puget Sound (Yount and Gower, 1991). Magnetic conglomerates in the Miocene Blakely Harbor Formation are described by Blakely *et al.* (2002). Fulmer (1975) described volcanic conglomerates within the Blakeley Formation. Currently we lack measurements of the magnetic susceptibilities for most of these conglomerates to test this hypothesis.

Multiple sources for these basaltic conglomerates are recognized. Eocene volcanic rocks (Fig. 1) are exposed east and west of the Puget Sound (Waldron, 1962; Haeussler and Clark, 2000) and lie at shallow depth on the southwestern flank of the Seattle uplift at the Hofert #1 well (Sceva, 1957). Uplift and subsequent denudation of Eocene volcanic rocks, consistent with our hypothesis, contributed to the magnetic properties of these Tertiary sedimentary rocks.

Paleomagnetic Evidence for Late Quaternary Folding on the Seattle Uplift

Paleomagnetic measurements on Pleistocene deposits sampled near sea level support late Quaternary growth of the Three Tree Point and Point Robinson anticlines (Hagstrum *et al.*, 2002). Although normally polarized sites are equivocal, tectonic uplift and erosion are needed to expose reversely magnetized sites older than the Brunhes-Matuyama transition at ~780 k.y. ago (Hagstrum *et al.*, 2002). Pleistocene growth of the Three Tree Point and Point Robinson anticlines is compatible with 10 reversed-polarity samples. Holocene uplift at Restoration Point is known from uplifted marine terraces (Bucknam *et al.*, 1992). In contrast, little late Quaternary fold growth is inferred between the Alki Point and Three Tree Point anticlines from five normal or transitional polarity sites (Hagstrum *et al.*, 2002).

Late Quaternary deformation along the Tacoma fault zone is concentrated on eastward-trending anticlines lying north of the Rosedale monocline rather than on the monocline itself. Late Quaternary deformation along the Tacoma fault/Point Robinson anticline (Fig. 1) is supported by four reversed-polarity sites (Hagstrum *et al.*, 2002) and by trenching of the Catfish Lake scarp (Sherrod *et al.*, 2003, 2004). In contrast, less late Quaternary uplift above the Rosedale monocline is consistent with the normal-polarity sites along it (Hagstrum *et al.*, 2002).

Geologic Observations of Quaternary Folding over the Seattle Uplift

Booth *et al.* (2004) mapped the strike and dip of Quaternary deposits at isolated coastal exposures along Puget Sound, showing that these deposits display a consistent fold axis orientation. They mapped eastward-trending folds having wavelengths no greater than a few kilometers. Locations of fold axes inferred by Booth *et al.* (2004) show intriguing correlation to those inferred from the seismic profiles, especially along the North Point Robinson anticline.

Discussion

Passive-Roof Duplexes

Although the proposed passive-roof duplex model for the Seattle uplift is new, similar structural interpretations are commonly proposed elsewhere. Passive-roof duplexes, or triangle zones (Figs. 3 and 9; Jones, 1996b), are commonly imaged at deformation fronts of fold-and-thrust belts, including the Great Valley of California, the Kirthar thrust belt of Pakistan, Papuan fold belt of New Guinea, the Pyrenees, and the Canadian Cordillera (e.g., Banks and Warburton, 1986; Cooper, 1996; Medd, 1996).

Several suitable detachment surfaces required for triangle zone formation (Couzens and Wiltschko, 1996; Sans *et al.*, 1996) appear to be present in the Seattle basin. Our inferred roof thrust in part lies at the top of the Eocene volcanic rocks and base of the Tertiary sedimentary rocks, where a large mechanical contrast might be expected. Fulmer (1975) mapped massive micaceous shales at the base of exposures of the mainly Upper Eocene and Oligocene Blakeley Formation along Waterman Point that could represent a potential detachment surface higher in the stratigraphic column (Fig. 2). Siltstones within the Blakeley Formation (Yount and Gower, 1991) may provide other suitable detachment surfaces. Exposures of Blakeley Formation within and to the south of this belt (Waldron, 1962) are consistent with a decollement within or beneath it. Still higher in the column, the base of the Blakely Harbor Formation is a poorly exposed dark carbonaceous siltstone (Yount and Gower, 1991) that represents a potential detachment surface. It is possible that one or more of these possible detachment surfaces could be currently accommodating the north–south compression in the Puget Lowland.

Our preferred structural cross section across the Seattle uplift (Fig. 10) exhibits several similarities (and some differences) in structural style and scale of deformation to those inferred for the Kirthar thrust belt in the vicinity of Bolan Pass, central Pakistan (Fig. 9) (Banks and Warburton, 1986). The similarities include, as for the Seattle uplift, a roof thrust about 15–20 km long. The thickness of the Kirthar molasse trough, nearly 10 km, is close to the thickness of the Seattle basin (Brocher *et al.*, 2001). As in the Seattle basin, out-of-syncline intra-molasse detachments, 15–20 km long, of relatively minor displacement are inferred in the Kirthar molasse trough. Another possible similarity is that the roof thrust may be faulted by imbricate thrusting along F12 at Three Tree Point as in the Kirthar thrust belt. One interesting potential difference is that in the Kirthar molasse trough the intra-molasse detachment surfaces have no direct connection to the master thrust.

Geometry of the Floor and Imbricate Thrusts

Two northward-trending sections in the Puget Lowland show the inferred geometry of the floor thrusts at depth (Fig. 10). The floor thrust of the Seattle fault steepens with depth from the wedge tip, reaching a maximum of about 35° (Fig. 10B). South-dipping fault-plane reflections provide evidence for at least three other imbricate fault strands within the inferred Eocene volcanic basement; variations in structural relief of the reflector thought to originate from the Blakeley Formation also provide evidence for these faults (Figs. 7 and 8). These fault planes dip throughout most of their mapped lengths (to 10 or 12 km) between 30° and 35°. Pratt *et al.* (1997) estimated the dip of the Seattle fault below about 5 km as 20° ± 5° (Fig. 10A), slightly less than that estimated here. ten Brink *et al.* (2002) estimated the dip as 35° to 40°, close to our estimate. The floor fault inferred here is 2 km deeper than previously interpreted (Pratt *et al.*, 1997; ten Brink *et al.*, 2002), and we correlate faint reflections noted by these workers with this fault.

Along the Puget Sound just west of Seattle (Fig. 10B), the dip of the floor thrust is approximately constant to a depth of at least 18 to 20 km. The dip is constrained by the observation of fault plane reflections to a depth of 10 to 12 km and also matches the depth and focal mechanism of the Point Robinson earthquake (Dewberry and Crosson, 1996). The focal mechanism for the Bremerton earthquake appears most consistent with bedding-plane slip along a detachment at the base of the Tertiary sedimentary rocks in the Seattle basin and the top of the Crescent Formation (Fig. 10B), although given its uncertainty in depth we cannot rule out the possibility that this earthquake occurred along a shallower bedding plane or even on the floor thrust.

In Figure 10B and C, the floor thrust of the Tacoma fault system is shown as a north-dipping backthrust that intersects the floor thrust of the Seattle fault at a depth of about 12 km. Overthrusting of the Tacoma basin along the western end of the Tacoma fault (Fig. 10C) is largely inferred by analogy with the Seattle fault geometry (Fig. 10B) and is consistent with a reversal with depth seen in seismic tomography velocities (Brocher *et al.*, 2001). There are currently no other geophysical constraints on the dip of the floor thrust of the Tacoma fault zone. For this reason, we show comparable dips for the floor thrusts in the Tacoma and Seattle faults (about 35°). Along strike variations in the location of the wedge tip along the Tacoma fault and the westward increase in structural relief along the fault (Fig. 10C) are inferred from tomography seismic velocity models (Fig. 6) and gravity inversions (Brocher *et al.*, 2001; Parsons *et al.*, 2001).

Geometry of the Roof Thrusts

Our northward-trending cross section centered on the Catfish Lake scarp and Gold Mountain (Fig. 11) shows a shoaling of the top of Eocene volcanic rocks based on the Hofert #1 well (Sceva, 1957) and on exposure of the Crescent Formation volcanics (Haeussler and Clark, 2000). Tomography models (Brocher *et al.*, 2001) indicate that the Seattle basin is 4–5 km thinner, the Tacoma basin is 4–5 km thicker, and the top of the Eocene volcanic rocks is about 2 km shallower along the Seattle uplift along this cross-section than along Puget Lowland (Fig. 10C). Proposed mechanisms for the higher structural elevation of the Eocene volcanic basement along the uplift include west-directed thrusting along the Hood Canal and other faults bounding the Olympic Mountains and the lowland (B. Sherrod, personal communication, 2003) and flexure of the Crescent terrane produced by underthrusting of the Olympic core complex (Crosson and Symons, 2001).

Shallower Eocene volcanic basement along the western Seattle uplift (Fig. 10C) implies that very little of the hanging wall remains (Fig. 11). Perhaps, as a consequence, along the western half of the uplift most of the surface deformation appears to be focused at the leading edges of the uplift: on Catfish Lake scarp, at the southern end of the uplift, and on the Toe Jam Hill fault, at the northern end of the uplift (Fig. 1).

Geometry of the Western End of the Tacoma Fault Zone

Seismic lines image the Rosedale monocline (Johnson *et al.*, 2004) defining the triangle zone and the tip of the wedge along the eastern end of the Tacoma fault zone. The geometry of the Tacoma fault zone at its western end, however, is not constrained by comparable seismic lines. Seismic lines in Case Inlet image a probable fault located several kilometers south of the Catfish Lake scarp (Johnson *et al.*, 2004; Sherrod *et al.*, 2004), suggesting that the tip of the wedge lies well south of lineament C (Fig. 6C). The tip of the wedge shown in Figure 1 thus lies well south of the Tacoma fault as defined by Johnson *et al.* (2004), but it is otherwise poorly constrained.

How Does the New Interpretation Differ from Earlier Interpretations?

Pratt *et al.* (1997), recognizing the Blake Island, Three Tree Point, and Point Robinson anticlines (which they labeled A, B, and C), proposed that they originated from south-dipping small splays from a single, deep, south-dipping master thrust (Fig. 10A). They suggested that the south-dipping splay faults ruptured the surface only at the Alki/Restoration Point anticline and that the other shallow anticlines formed as fault-propagation folds (Fig. 10A). We interpret these and smaller shallow anticlines as originating from splay thrusting above a shallow roof thrust because their short wavelengths may be more easily explained by a shallow detachment.

We differ from Pratt *et al.* (1997), Johnson *et al.* (1999),

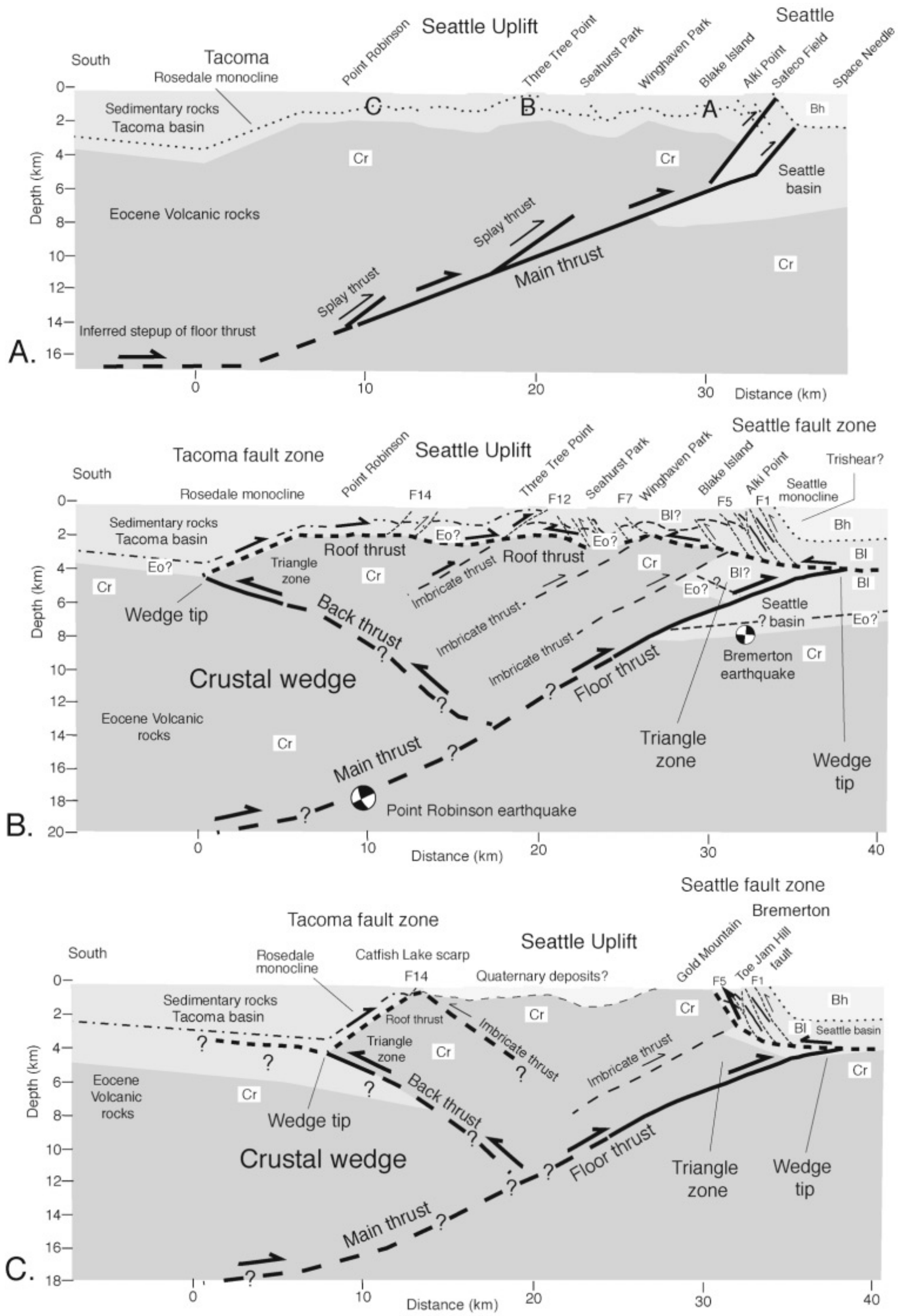

Figure 10. Schematic structural cross section along the Puget Sound, based on Figures 7 and 8, showing possible geometry of roof, imbricate, and floor thrusts. (A) Cross section modified from Pratt *et al.* (1997). (B) Cross section from this study, showing splay thrusts (F1 to F14), roof thrusts, imbricate thrusts, triangle zones, and floor thrusts in Puget Sound (Fig. 10). Differently patterned lines within inferred Tertiary sedimentary rocks over the Seattle uplift may or may not be correlative, so different patterns are used for them. Focal mechanisms for the 1997 Bremerton and 1995 Point Robinson earthquakes (Dewberry and Crosson, 1996; Blakely *et al.*, 2002) are superimposed. (C) Cross section from this study for a section through the Catfish Lake scarp, the Hofert #1 well, and Gold Mountain (Fig. 11). Abbreviations: Bh, Blakely Harbor Formation; Bl, Blakeley Formation; Eo, Eocene sedimentary rocks; Cr, Crescent Formation.

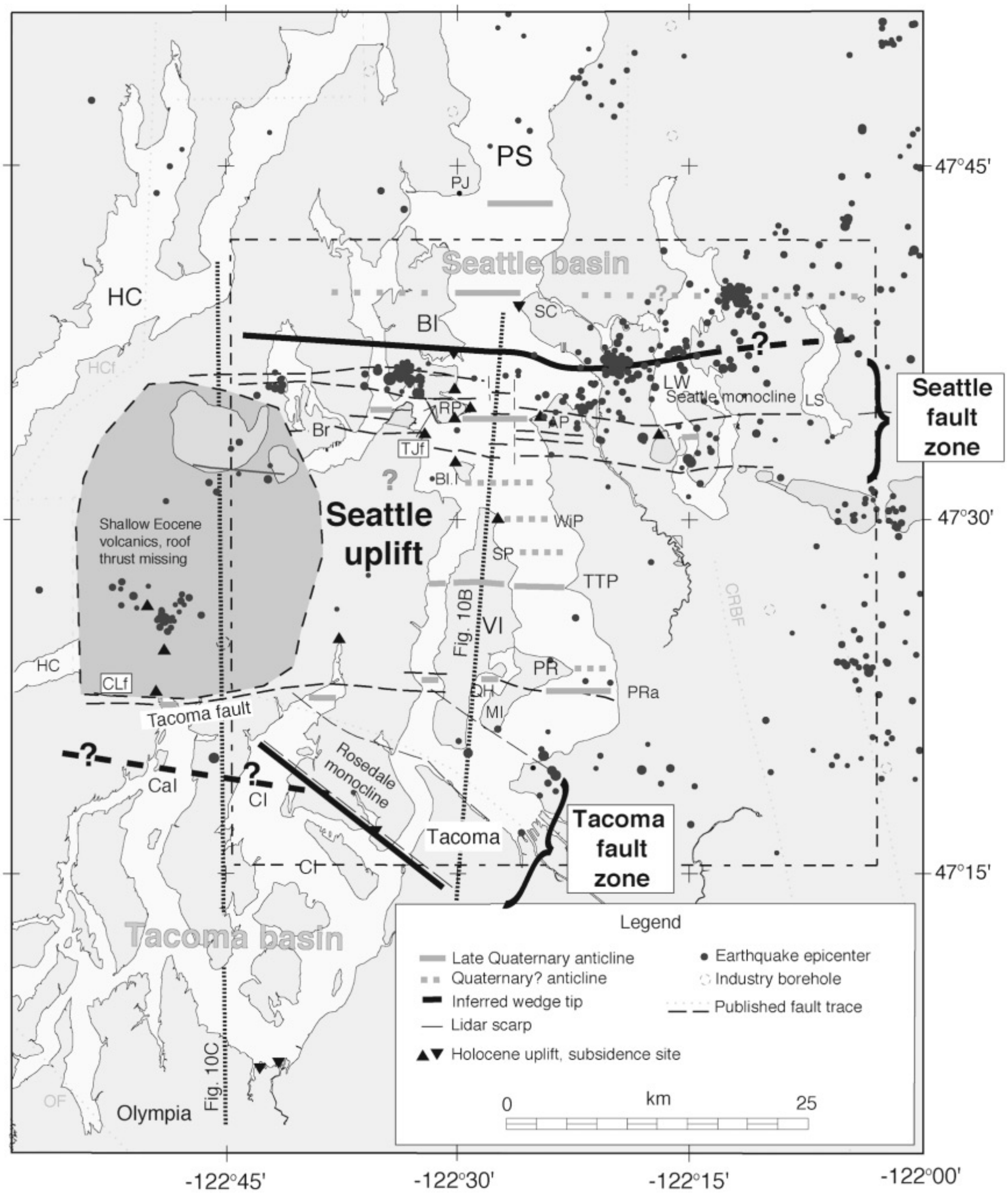

Figure 11. Comparison of seismicity for the upper 8 km of the crust (black dots) with the location of the anticlines and wedge tips described here. Seismicity is plotted for 1970 through 2002, for magnitudes 1.0 to 4.7, and for the region north of 47°15′N. Format as for Figure 1. Dashed rectangle shows region of seismicity projected onto Figure 8.

and ten Brink *et al.* (2002) in interpreting the Seattle fault as a triangle zone (Fig. 3C) rather than as a propagating fault (Fig. 3A). We also differ from Pratt *et al.* (1997) in suggesting that there may be south-dipping imbricate thrusts beneath the Seattle uplift (Fig. 10B), with the floor faults along the Seattle and Tacoma faults representing the most active fault strands.

We agree with Johnson *et al.* (1999) and Calvert *et al.* (2001, 2003) that several faults produce the structural relief in the Alki/Restoration Point anticline. Johnson *et al.* (1999) considered this structure to be an anticlinal or high-angle breakthrough fault in a fault-propagation fold (Fig. 3A). Instead, we prefer to interpret the faults near Alki Point as mainly short, north-dipping thrusts splaying upward from a shallow roof thrust.

For the Seattle fault, our interpretation of the wedge tip places the subsurface "deformation" front about 3 km farther north than the surficial "deformation" front mapped by Johnson *et al.* (1999) and Blakely *et al.* (2002) but within 1 km of the wedge tip location proposed by ten Brink *et al.* (2002). Our interpretation does not require segmentation of the floor and roof thrusts. Proposed segmentation of the shallow north-dipping splay thrusts along the Seattle fault (Johnson *et al.*, 1999) can be explained either by *en echelon* stepovers of the near-surface splay thrusts soling into the underlying roof thrust or by minor tear faults that also root into the roof thrust.

Johnson *et al.* (2004) envision the western end of the Tacoma fault as a north-dipping backthrust very similar to that of Figure 10B, consistent with recent trenching results (Sherrod *et al.*, 2003, 2004). We extend this fault farther to the southeast (Fig. 10B), and we explain F14 in Puget Sound as a south-dipping splay thrust soling into a shallow roof thrust. Johnson *et al.* (2004) interpreted F14 as a segment of a high-angle eastward-trending fault (the Tacoma fault) with a potentially significant component of lateral slip and vertical extent.

We share the view of ten Brink *et al.* (2002) that shallow south-directed thrusting is important along the Seattle uplift. ten Brink *et al.* (2002) showed that models for the coseismic uplift and subsidence for the latest event about 1100 years ago require shallow south-directed thrusting. Given the relative inactivity of splay faults F5 to F7, it seems reasonable to infer that only the northernmost 10 km of the roof thrust ruptured during the most recent large Seattle fault earthquake, as modeled by ten Brink *et al.* (2002).

Finally, we differ from Brocher *et al.* (2001) by suggesting that the floor thrust has a low dip (30°) rather than a steeper dip (60°–80°). Our interpretation is consistent with the tomography models but, like Blakely *et al.* (2002) and ten Brink *et al.* (2002), we argue that the microseismicity suggesting a steeper dip does not occur along the floor thrusts of the Seattle and Tacoma fault zones.

Seismic Hazard Implications of a Passive-Roof Duplex System

Surficial deformation from central Seattle to Three Tree Point (a distance of ~18 km) is dominated by shallow, south-directed splay thrusting and folding, consistent with trenching results from the Toe Jam Hill and the Waterman Point fault scarps (Nelson *et al.*, 2002, 2003a,b). These Holocene scarps all result from up-to-the-north, south-directed thrusting. Between Three Tree Point and Tacoma, surface deformation is dominated by shallow, north-directed splay thrusting that roots into a roof thrust over the Tacoma fault zone. Two-way travel times indicate that the depth to the roof thrusts lies between 1.2 and 2.2 km. Holocene folding over a north-dipping thrust along the Tacoma fault was found at the Catfish Lake scarp (Sherrod *et al.*, 2003, 2004).

South-directed thrusts near Alki/Restoration Point, Three Tree Point, and Point Robinson, the only late Quaternary thrusts in the shallow splay thrust system, deform the seafloor. South-directed thrusts between Alki/Restoration and Three Tree Points do not demonstrate late Quaternary activity and may be aseismic, reflecting the northward progression and evolution of the duplex structure and of its roof thrusts (Fig. 12).

We interpret these shallow splay thrusts as passive structures, slipping only during motion on the underlying roof and floor thrusts. If this is the case, ages of soil offsets measured at fault-scarp trenches can be used to date ruptures of the floor thrusts. Models of coseismic uplift suggest that splay thrusts F1 to F4 and possibly F5 as well as the roof and floor thrust slipped in the last major rupture of the Seattle fault zone about 1100 years ago (ten Brink *et al.*, 2002). If these splay thrusts have a depth extent of a few kilometers (Fig. 10B) and are a few tens of kilometers long as suggested by the continuity of associated magnetic anomalies (Fig. 6C), coseismic slip along them during rupture of the floor thrust may have produced additional seismic moment equivalent to a magnitude of 6 (Wells and Coppersmith, 1994).

In our view there is permissive seismic evidence that the Seattle basin is underlain by one or more detachments. The wedge-tip model does not require these thrusts, and, in any case, the amount of slip in the Seattle basin north of the Seattle monocline is probably small. The detachment plane is presumably weak, so thrusting in the Seattle basin is probably passive. This view is supported by the relative absence

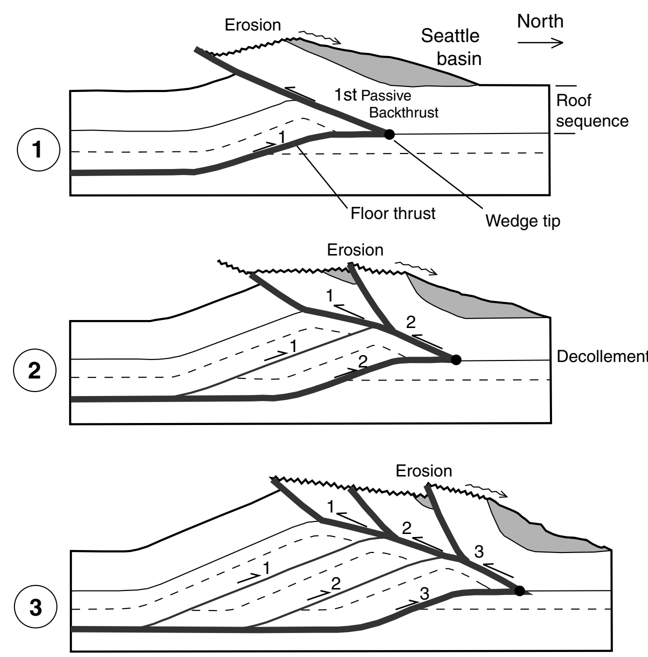

Figure 12. Proposed structural evolution of the northern end of the Seattle uplift, modified from Banks and Warburton (1986). Three stages of the evolution of the duplex illustrate its northward propagation. Active segments of the floor and roof thrusts are highlighted by thicker dark gray lines.

of seismicity along the inferred thrust north of the wedge tip (Figs. 8 and 11). If the Bremerton earthquake hypocenter lies along the base of the Tertiary basin fill, as shown in Figure 10B, then detachment faulting in the basin may not be entirely passive.

An additional hazard may be posed by updip-directed rupture that focuses radiated seismic waves toward the surface, a phenomena commonly observed in thrust faulting (Somerville *et al.*, 1997). Tomography and gravity data (Fig. 6) indicate that Seattle sits astride the deepest portion of the Seattle basin (Brocher *et al.*, 2001; Parsons *et al.*, 2001; Snelson, 2001; Van Wagoner *et al.*, 2002), which is known to amplify weak ground motions at periods of around 3 sec (Pratt *et al.*, 2003).

We believe that the floor thrust of the Seattle fault is the most important thrust beneath Seattle (Fig. 12) because models for the coseismic uplift from the *M* 7 Seattle fault earthquake 1100 years ago suggests that this was the only south-dipping thrust to rupture (ten Brink *et al.*, 2002). This inference is consistent with the high rate of microseismicity along its northern wedge tip (Figs. 8 and 11) and with the absence of microseismicity along the other, possibly abandoned, wedge tips defined by imbricate thrusts. Small, shallow-focus earthquakes observed in the Seattle basin, directly above the wedge tip, may reflect bedding plane slip or trishear above the wedge tip, or may, within probable depth errors (Brocher *et al.*, 2003), lie at the wedge tip (Fig. 8). Beneath 8 km depth the inferred imbricate and floor thrusts are aseismic (not shown).

Tacoma overlies the Rosedale monocline (Fig. 4F), which reflects southward thrusting of the wedge tip (Fig. 10B). Tacoma, like Seattle, is built atop a thick Cenozoic sedimentary basin (e.g., Brocher *et al.*, 2001), and ground motions there from future large earthquakes on the Tacoma fault will be enhanced by source directivity and basin amplification (T. L. Pratt and T. M. Brocher, in preparation, 2004). The upper portion of the floor thrust in the Tacoma fault zone is currently aseismic (Fig. 11).

Amount of North–South Shortening and Vertical Slip on the Seattle Fault Floor Thrust

The north–south shortening measured at the top of the Crescent volcanic rocks along the floor thrust and northernmost imbricate thrust is about 13 km. This estimate was obtained from a migrated, depth-converted seismic line in Puget Sound (Fig. 7). The calculated north–south shortening rate since 15 m.y.a (ten Brink *et al.*, 2002), about 0.9 mm/yr, is similar to the 0.7–1.1 mm/yr slip rate estimated by Johnson *et al.* (1999) and the 0.7–0.9 mm/yr slip rate calculated for the Seattle fault by ten Brink *et al.* (2002). Booth *et al.* (2004) inferred 0.25–1 mm/yr of north–south shortening on the basis of folding of late Quaternary strata along Puget Sound.

The total vertical slip predicted for this north–south shortening, assuming a fault dip of 35°, is 7.5 km, which is close to the observed total offset of Eocene volcanic basement (Fig. 10B). If we assume that the 4.5-km separation in depth observed between the dashed and dotted horizons in the Tertiary sedimentary sequence in the Seattle basin (Fig. 10B) is also appropriate to the south of the Seattle fault zone, this separation suggests that these Miocene rocks would now be 3–4 km above sea level south of the fault. Based on this assumption, we infer that the Miocene sedimentary rocks (dotted horizon in Fig. 10B) have been uplifted between 5 and 6 km, suggestive of a minimum uplift rate of 0.3 mm/yr and a maximum uplift rate of 0.4 mm/yr for the past 15 m.y.

Amount of North–South Shortening on Roof Thrust

Shortening accommodated by roof thrusting along the Seattle fault zone was determined from the length of Tertiary sedimentary horizons in a migrated, depth-converted seismic line in Puget Sound (Fig. 8C). A minimum of 4.5 km of shortening was measured from the Seattle fault wedge tip south to Point Robinson in two separate Tertiary sedimentary horizons. Assuming an age of 13.3 m.y. for the unconformity at the top of the Oligocene to the Eocene Blakeley Formation, as suggested by ten Brink *et al.* (2002), we calculate a north–south shortening rate of 0.34 mm/yr for the northern and central parts of the uplift; most shortening occurs near Alki/Restoration Point. This rate underestimates the slip rate because an unknown length of the dotted reflector has been eroded during the uplift of the Alki/Restoration Point anticline (Fig. 10B); it overestimates the rate because the dashed Oligocene reflector is older than 13.3 m.y. Despite these caveats, our shortening rate for the roof thrust closely agrees with the slip rate determined from offset soils at the Toe Jam Hill fault (Nelson *et al.*, 2003b).

Widespread Vertical Offset at About 1100 Years Ago

Our proposed geometry of the floor and roof thrusts (Fig. 10B and C) may account for observations of widespread rapid uplift and subsidence of coastal marsh deposits in central Puget Sound about 1100 years ago (Bucknam *et al.*, 1992; Sherrod, 2001; Sherrod *et al.*, 2003, 2004). Slip on the main thrust of the crustal wedge, say between km 0 to 15 on Figure 10B and C, will result in regional uplift. This motion could be accommodated by slip on either or both of the floor thrusts and roof thrusts along the Seattle and Tacoma fault zones. Hence, the temporal coincidence of uplift at both ends of the Seattle uplift could be a natural consequence of the duplex geometry. Slip on this master floor thrust system can result in a large, *M* 7 to 7.5, earthquake (Pratt *et al.*, 1997).

Summary

We hypothesized that the Seattle fault is the leading edge of a northward propagating fold-and-thrust belt and that the Tacoma fault is the trailing edge of the same doubly vergent fold belt. Seismic lines reveal prominent monoclines in the Seattle and Tacoma basins along the frontal part of the Seattle and Tacoma fault zones, which we interpret as evidence for triangle zones along both fault zones. Slip on the floor thrusts would produce regional uplift along these fault zones.

In our interpretation the Seattle uplift along Puget Sound is underlain at shallow depth (1–2 km) by a passive-roof duplex system containing 14 small splay thrusts (F1 to F14), at least 3 of which show Holocene offset in fault-scarp trenches. In our view, this roof thrust system accommodates the northward propagation of the triangle zone into the Seattle basin. The active tip of the wedge that currently underlies Seattle is blind and is located about 3 km farther north beneath Seattle than previously recognized. On the basis of water well control and structural relations, we interpret minor arches imaged by the seismic data in the Seattle basin as folding associated with minor slip along the master floor thrust.

The splay thrusts that sole into a shallow roof thrust are not expected to rupture independently of the roof and floor thrusts (Jones, 1996b). Thus, in principle, dates of slip obtained from them should provide information on the ruptures of the roof and floor thrusts. Comparison of ages of regional uplift events resulting from slip on the floor thrusts versus ages of splay faulting inferred from trench excavations should permit testing of this hypothesis. The shallow splay thrusts pose an earthquake hazard from more localized uplift and folding of the surface during coseismic slip of the roof and floor thrusts.

The passive-roof duplex hypothesis can be tested in several ways. For example, the notion that a roof thrust lies along the contact between Tertiary sedimentary rocks and the top of the Crescent Formation may be tested by examination of this contact where exposed at the western end of the uplift (Fig. 1). Measurements of the magnetic susceptibility of Tertiary volcanic conglomerates will permit refinement and testing of magnetic models. The Three Tree Point anticline is inferred to place Tertiary sedimentary rocks near the surface, making them and the inferred shallow splay thrusts accessible via shallow drilling and coring. Reprocessing SHIPS data to account for actual shotpoint locations and streamer feathering should yield better images of the key divergent reflections defining triangle zones. New, higher quality seismic lines crossing the Seattle and especially the Tacoma faults with smaller line spacings may help define the along strike variability of these faults and provide data needed for rigorous reconstruction of the fault history.

Acknowledgments

Sam Johnson provided copies of the industry lines. Andy Calvert plotted seismic sections of the SHIPS data. Conversations with Tom Moore, Dan O'Connell, and Brian Sherrod helped crystallize key elements of the structural interpretation. Brian Sherrod provided Figure 4C. Andy Calvert, Jonathan Hughes, Tatsuya Ishiyama, Sam Johnson, Mark Molinari, Alan Nelson, Chris Potter, Tom Pratt, Brian Sherrod, and Cathy Snelson reviewed earlier drafts of the manuscript.

References

Atwater, B. F. (1999). Radiocarbon dating of a Seattle earthquake to A.D. 900–930, Washington, *Seism. Res. Lett.* **70,** 232.

Banks, C. J., and J. Warburton (1986). 'Passive-roof' duplex geometry in the frontal structure of the Kirthar and Sulaiman mountain belts, Pakistan, *J. Struct. Geol.* **8,** 229–237.

Blakely, R. J., R. E. Wells, C. S. Weaver, and S. Y. Johnson (2002). Location, structure, and seismicity of the Seattle fault, Washington: evidence from aeromagnetic anomalies, geologic mapping, and seismic-reflection data, *Geol. Soc. Am. Bull.* **114,** 169–177.

Booth, D. B., K. G. Troost, and J. T. Hagstrum (2004). Deformation of Quaternary strata and its relationship to crustal folds and faults, south-central Puget Lowland, Washington State, *Geology* **32,** 505–508.

Brocher, T. M., and A. L. Ruebel (1998). Compilation of 29 sonic and density logs from 23 oil test wells in western Washington State, *U.S. Geol. Surv. Open-File Rept. 98-249*, 41 pp.

Brocher, T. M., T. Parsons, R. J. Blakely, N. I. Christensen, M. A. Fisher, R. E. Wells, and the SHIPS Working Group (2001). Upper crustal structure in Puget Lowland, Washington: results from 1998 Seismic Hazards Investigation in Puget Sound, *J. Geophy. Res.* **106,** 13,541–13,564.

Brocher, T. M., C. S. Weaver, and R. S. Ludwin (2003). Assessing hypocentral accuracy and lower magnitude completeness in the Pacific Northwest using seismic refraction detonations and cumulative frequency–magnitude relationships, *Seism. Res. Lett.* **74,** 772–789.

Buchanan-Banks, J. M., and D. S. Collins (1994). Map showing depth to bedrock in the Tacoma and part of the Centralia 30′ × 60′ quadrangles, Washington, U.S. Geol. Surv. Misc. Field Studies Map MF-2265, 2 sheets, scale 1:100,000.

Bucknam, R. C., E. Hemphill-Haley, and E. B. Leopold (1992). Abrupt uplift within the past 1700 years at southern Puget Sound, Washington, *Science* **258,** 1611–1614.

Calvert, A. J., M. A. Fisher, and the SHIPS Working Group (2001). Imaging the Seattle fault zone with high-resolution seismic tomography, *Geophys. Res. Lett.* **28,** 2337–2340.

Calvert, A. J., M. A. Fisher, S. Y. Johnson, and the SHIPS Working Group (2003). Along-strike variations in the seismic velocity structure of the Seattle fault zone beneath Puget Sound, *J. Geophys. Res.* **108,** no. B1, 2005, doi 10.1029/2001JB001703.

Castonguay, S., and R. A. Price (1995). Tectonic heredity and tectonic wedging along an oblique hanging wall ramp: the southern termination of the Misty thrust sheet, southern Canadian Rocky Mountains, *Geol. Soc. Am. Bull.* **107,** 1304–1316.

Cooper, M. (1996). Passive-roof duplexes and pseudo-passive-roof duplexes at mountain fronts: A review, *Bull. Can. Pet. Geol.* **44,** 410–421.

Couzens, B. A., and D. V. Wiltschko (1996). The control of mechanical stratigraphy on the formation of triangle zones, *Bull. Can. Pet. Geol.* **44,** 165–179.

Crosson, R. S., and N. P. Symons (2001). Flexural origin of the Puget basins: implications for the Seattle fault and Puget basin tectonics (abstract), *EOS* **82,** no. 47, F856.

Dewberry, S. R., and R. S. Crosson (1996). The M_D 5.0 earthquake of January 29, 1995, in the Puget Lowland of western Washington: an event on the Seattle fault?, *Bull. Seism. Soc. Am.* **86,** 1167–1172.

Fisher, M. A., T. M. Brocher, R. D. Hyndman, A. M. Tréhu, C. S. Weaver, K. C. Creager, R. S. Crosson, T. Parsons, A. K. Cooper, D. Mosher, G. Spence, B. C. Zelt, P. T. Hammer, U. ten Brink, T. L. Pratt, K. C. Miller, J. R. Childs, G. R. Cochrane, S. Chopra, and R. Walia (1999). Seismic survey probes urban earthquake hazards in Pacific Northwest, *EOS* **80,** 13–17.

Fisher, M. A., R. D. Hyndman, S. Y. Johnson, R. S. Crosson, U. S. ten Brink, A. J. Calvert, T. M. Brocher, R. E. Wells, and the SHIPS Working Group (2004). Crustal structure and earthquake hazards of the subduction zone in the central part of Cascadia, *U.S. Geol. Surv. Prof. Pap.* 1661-X (in press).

Fulmer, C. V. (1975). Stratigraphy and paleontology of the type Blakeley and Blakely Harbor Formations, in *Conf. on Future Energy Horizons* of the Pacific Coast, Paleogene Symp. and Selected *Tech. Pap. Am. Assoc. Petrol. Geol., Soc. Econ. Paleo. Miner., and Soc. Econ. Geophys., Annu. Meet., Pacific Sec., Proc.*, D. W. Weaver, G. R. Hornaday, and A. Tipton (Editors), 210–271.

Gower, H. D., J. C. Yount, and R. S. Crosson (1985). Seismotectonic map of the Puget Sound region, Washington, *U.S. Geol. Surv., Misc. Invest. Series Map I-1613*, scale 1:250,000.

Haeussler, P. J., and K. M. Clark (2000). Geologic map of the Wildcat lake 7.5′ quadrangle, Kitsap and Mason Counties, Washington, *U.S. Geol. Surv. Open-File Rep. 00-356*, scale 1:24,000, 1 sheet, http://geopubs.wr.usgs.gov/open-file/of00-356/.

Hagstrum, J. T., D. B. Booth, K. G. Troost, and R. J. Blakely (2002). Magnetostratigraphy, paleomagnetic correlation, and deformation of Pleistocene deposits in the south-central Puget Lowland, Washington, *J. Geophys. Res.* **107,** no. B4, EPM x-1 to x-13, doi 10.1029/2001JB000557.

Hyndman, R. D., S. Mazzotti, G. C. Rogers, and D. Weichert (2003). Frequency of large crustal earthquakes in Puget Sound–Southern Georgia Strait predicted from geodetic and geological deformation rates, *J. Geophys. Res.* **108,** no. B1, doi 10.1029/2001JB001710.

Johnson, S. Y., R. J. Blakely, W. J. Stephenson, S. V. Dadisman, and M. A. Fisher (2004). Active shortening of the Cascadia forearc and implications for seismic hazards of the Puget Lowland, *Tectonics* **23,** TC1011, doi 10.1029/2003TC001507.

Johnson, S. Y., S. V. Dadisman, J. R. Childs, and W. D. Stanley (1999). Active tectonics of the Seattle fault and central Puget Sound, Washington—Implications for earthquake hazards, *Geol. Soc. Am. Bull.* **111,** 1042–1053.

Johnson, S. Y., C. J. Potter, and J. M. Armentrout (1994). Origin and evolution of the Seattle fault and Seattle basin, Washington, *Geology* **22,** 71–74.

Jones, M. A. (1996a). Thickness of unconsolidated deposits in the Puget Sound Lowland, Washington and British Columbia, *U.S. Geol. Surv. Water Res. Invest. Rep. 94-4133*.

Jones, P. B. (1996b). Triangle zone geometry, terminology and kinematics, *Bull. Can. Pet. Geol.* **44,** 139–152.

McFarland, C. R. (1983). Oil and gas exploration in Washington, 1900–1982, Washington (State), *Dept. Nat. Res., Div. Geol. Earth Res. Inform. Circ.* **75,** 119 pp.

Medd, D. M. (1996). Recent triangle zone deformation in Papua New Guinea, *Bull. Can. Pet. Geol.* **44,** 400–409.

Miller, M., D. J. Johnson, C. M. Rubin, H. Dragert, K. Wang, A. Qamar, and C. Goldfinger (2001). GPS-determination of along-strike variations in Cascadia margin kinematics: implications for relative plate motion, subduction zone coupling, and permanent deformation, *Tectonics* **20,** 161–176.

Nelson, A. R., S. Y. Johnson, H. M. Kelsey, B. L. Sherrod, R. E. Wells, K. Okumura, L. A. Bradley, R. Bogar, and S. F. Personius (2003a). Field and laboratory data from an earthquake history study of the Waterman Point fault, Kitsap County, Washington, *U.S. Geol. Surv. Misc. Field Studies Map MF-2423*.

Nelson, A. R., S. Y. Johnson, H. M. Kelsey, R. E. Wells, B. L. Sherrod, S. K. Pezzopane, L. A. Bradley, and R. D. Koehler, III (2003b). Late Holocene earthquakes on the Toe Jam Hill fault, Seattle fault zone, Bainbridge Island, Washington, *Geol. Soc. Am. Bull.* **115,** 1388–1403.

Nelson, A. R., S. Y. Johnson, R. E. Wells, S. K. Pezzopane, H. M. Kelsey, B. L. Sherrod, L. A. Bradley, R. D. Koehler III, R. C. Bucknam, R. A. Haugerud, and W. T. LaPrade (2002). Field and laboratory data from an earthquake history study of the Toe Jam Hill fault, Bainbridge Island, Washington, *U.S. Geol. Surv. Open-File Rept. 02-60*, 37 pp., 2 plates.

Parsons, T., R. J. Blakely, and T. M. Brocher (2001). A simple algorithm for sequentially incorporating gravity observations in seismic traveltime tomography, *Int. Geol. Rev.* **43,** 1073–1086.

Pratt, T. L., T. M. Brocher, C. S. Weaver, K. C. Miller, A. M. Tréhu, K. C. Creager, R. S. Crosson, and C. M. Snelson (2003). Amplification of seismic waves by the Seattle basin, northwestern U.S., *Bull. Seism. Soc. Am.* **93,** 533–545.

Pratt, T. L., S. Johnson, C. Potter, W. Stephenson, and C. Finn (1997). Seismic reflection images beneath Puget Sound, western Washington state: the Puget Lowland thrust sheet hypothesis, *J. Geophys. Res.* **102,** 27,469–27,489.

Rau, W. W., and S. Y. Johnson (1999). Well stratigraphy and correlations, western Washington and northwestern Oregon, *U.S. Geol. Surv. Geol. Invest. Ser. Map I-2621*, 31 pp. 3 foldouts.

Sans, M., J. A. Munoz, and J. Verges (1996). Triangle zone and thrust wedge geometries related to evaporitic horizons (southern Pyrenees), *Bull. Can. Pet. Geol.* **44,** 375–384.

Sceva, J. E. (1957). Geological and ground-water resources, Kitsap County, Washington, *U.S. Geol. Surv. Water Supply Pap.* **1413,** 178 pp., 3 plates.

Sherrod, B. L. (1998). Late Holocene environments and earthquakes in southern Puget Sound, *Ph.D. Thesis*, University of Washington, 159 pp.

Sherrod, B. L. (2001). Evidence for earthquake-induced subsidence about 1100 years ago in coastal marshes of southern Puget Sound, Washington, *Geol. Soc. Am. Bull.* **113,** 1299–1311.

Sherrod, B. L., T. M. Brocher, C. S. Weaver, R. C. Bucknam, R. J. Blakely, H. M. Kelsey, A. R. Nelson, and R. Haugerud (2004). Holocene scarps near Tacoma, Washington, USA, *Geology*, **32,** 9–12.

Sherrod, B. L., A. Nelson, H. Kelsey, T. Brocher, R. Blakely, C. Weaver, N. Rountree, and S. Rhea (2003). Late Holocene deformation along the Tacoma fault zone, southern Puget Sound, Washington, *U.S. Geol. Surv. Open-File Rept. 03-455.*

Snelson, C. M. (2001). Investigating crustal structure in western Washington and in the Rocky Mountains: implications for seismic hazards and crustal growth, *Ph.D. Dissertation*, University of Texas El Paso, 234 pp.

Somerville, P. G., N. F. Smith, R. W. Graves, and N. A. Abrahamson (1997). Modification of empirical strong ground motion attenuation relations to include the amplitude and duration effects of rupture directivity, *Seism. Res. Lett.* **68,** 199–222.

Suppe, J. (1983). Geometry and kinematics of fault-bend folding, *Am. J. Sci.* **283,** 684–721.

Suppe, J., and D. A. Medwedeff (1990). Geometry and kinematics of fault-propagation folding, *Eclogae Geol. Helv.* **83,** 409–454.

ten Brink U. S., P. C. Molzer, M. A. Fisher, R. J. Blakely, R. C. Bucknam, T. Parsons, R. S. Crosson, and K. C. Creager (2002). Subsurface geometry and evolution of the Seattle fault zone and the Seattle basin, Washington, *Bull. Seism. Soc. Am.* **92,** 1737–1753.

Van Wagoner, T. M., R. S. Crosson, K. C. Creager, G. F. Medema, L. A. Preston, N. P. Symons, and T. M. Brocher (2002). Crustal structure and relocated earthquakes in the Puget Lowland, Washington from high resolution seismic tomography, *J. Geophys. Res.* **107,** no. B12, 2381, doi 10.1029/2001JB000710.

Waldron, H. H. (1962). Geology of the Des Moines Quadrangle, Washington, *U.S. Geol. Surv. Geol. Quad. Map GQ-159*, scale 1:24,000.

Wells, D. L., and K. J. Coppersmith (1994). New empirical relationships among magnitude, rupture length, rupture width, rupture area, and surface displacement, *Bull. Seism. Soc. Am.* **84,** 974–1002.

Wells, R. E., C. S. Weaver, and R. J. Blakeley (1998). Fore-arc migration in Cascadia and its neotectonic significance, *Geology* **26,** 759–762.

Yount, J. C., and H. D. Gower (1991). Bedrock geologic map of the Seattle 30′ by 60′ quadrangle, Washington, *U.S. Geol. Surv. Open-File Rept. 91-147*, scale 1:100,000, 37 pp., 4 plates.

Yount, J. C., G. R. Dembroff, and G. M. Barats (1985). Map showing depth to bedrock in the Seattle 30′ by 60′ quadrangle, Washington, *U.S. Geol. Surv. Misc. Field Studies Map MF-1692*, scale 1:100,000.

U.S. Geological Survey
345 Middlefield Road
MS 977
Menlo Park, California 94025

Manuscript received 9 September 2003.